Uncoupling of Circadian Oscillators in the Central Extended Amygdala from the Master Clock During Stable Entrainment to an 'Exotic' Light Cycle

Valerie Harbour

A Thesis

in

The Department of

Psychology

Presented in Partial Fulfillment of the Requirements for the Degree of Master of Arts at

Concordia University

Montreal, Quebec, Canada

August 2007

Your file Votre référence
ISBN: 978-0-494-34748-5
Our file Notre référence
ISBN: 978-0-494-34748-5

ABSTRACT

Uncoupling of Circadian Oscillators in the Central Extended Amygdala from the Master Clock During Stable Entrainment to an 'Exotic' Light Cycle

Valerie Harbour

The circadian clock in the hypothalamic suprachiasmatic nucleus (SCN) can be entrained by light cycles longer than the normal 24-h light cycle, but little is known about the effect of such exotic light cycles on circadian clocks outside the SCN. The present thesis sought to examine the effect of exposure to a 26-h light-dark (LD) T-cycle (T26; 1-h-25-h LD) on the expression of the clock protein PERIOD2 (PER2) in the SCN and four regions of the limbic forebrain known to exhibit circadian oscillations in PER2 expression, the oval nucleus of the bed nucleus of the stria terminalis (BNSTov), central nucleus of the amygdala (CEA), basolateral amygdala (BLA), and dentate gyrus (DG). Control rats housed under a 24h T-cycle (T24; 1-h-23-h LD) and rats housed under the T26 cycle showed stable entrainment of wheel-running activity rhythms. As previously shown, PER2 expression in the SCN was also stably entrained in all T24 and T26-housed rats, peaking at the beginning of the active phase of the cycle. In contrast, exposure to the T26 LD cycle for 30 and 60 days, uncoupled the rhythm of PER2 expression in the BNSTov and CEA from the SCN, whereas PER2 rhythms in the BLA and DG were mostly unaffected. These results show that exposure to exotic light cycles can uncouple circadian oscillators in the limbic forebrain from the master SCN clock and suggest that such cycles may be used to study the functional consequences of disruptions in the phase relationship between the SCN and subordinate oscillators.

ACKNOWLEDGMENTS

I would like to thank my supervisor, Dr. Shimon Amir, for his continuous support and guidance. His enthusiasm and drive for scientific discoveries in circadian rhythms has impacted my way of thinking and has helped me set new personal goals.

I would also like to thank Dr. Barbara Woodside for taking the time to meet with me numerous times to go over the content and organization of my thesis, and also for her support.

Thank you to Dr. Jane Stewart for taking the time to read my thesis and help with the writing process.

Thank you to Barry Robinson for teaching me the techniques necessary for the study of circadian rhythms, and for his help on the experiments conducted for the present thesis.

I am lucky to have continuous support and guidance from many colleagues and friends. Thank you especially to Elaine Waddington Lamont and Natalina Salmaso for their help during this process and for their friendship. You are the best. Thank you also to Yannick Breton for his help with statistics and for his support.

Thank you to my parents, Stephen and Lucie, and my grandparents, Ina, Percy, Madelaine, and Gérard for their constant support and love.

Last but definitely not the-least, thank you to Christian Beaulé for his support, guidance, friendship, and love. I appreciate everything you do for me.

TABLE OF CONTENTS

LIST OF FIGURES

LIST OF TABLES

INTRODUCTION

Animals exhibit daily rhythms in fundamental physiological and behavioral processes. These rhythms are generated by molecular circadian clocks and synchronized by the environmental light cycle and other cyclic events, such as daily scheduled feeding (Challet, Caldelas, Graff, & Pevet, 2003; Masubuchi, Kataoka, Sassone-Corsi, & Okamura, 2005; Stephan, 2002). In mammals, a light-entrainable circadian clock located in the suprachiasmatic nucleus (SCN) regulates circadian behavioral and physiological rhythms by synchronizing central and peripheral subordinate oscillators (Lowrey & Takahashi, 2000). Although a great deal is known about the molecular programs responsible for the generation of circadian rhythms at the cellular and tissue levels (Ko & Takahashi, 2006; Lowrey & Takahashi, 2000), the mechanisms that mediate the synchronization between the light-entrainable SCN clock and subordinate oscillators in the brain and in multiple peripheral organs and tissues are not well understood. Our laboratory has previously studied this issue by evaluating the rate of re-entrainment of expression of the clock protein PERIOD2 (PER2) in the SCN and limbic forebrain in rats subjected to a single large (8-h) delay or advance shift in the entraining 12-h:12-h light-dark (LD) cycle. Under these conditions the light-induced phase adjustment in PER2 expression in the SCN was fast, preceding re-entrainment of locomotor activity rhythms, whereas that in a limbic structure, the oval nucleus of the bed nucleus of the stria terminalis (BNSTov) was delayed, suggesting weak coupling between the BNSTov oscillator and the light-entrained SCN clock (Amir, Lamont, Robinson, & Stewart, 2004).

It has been shown that locomotor activity (Stephan, 1983) and PER2 expression (Beaule, Houle, & Amir, 2003) in the SCN remain stably entrained in rats housed under a

long (26-h) LD cycle, demonstrating the high potential for plasticity in the mechanism mediating photic entrainment of the SCN clock under these conditions. To study the strength of the coupling between the SCN clock and subordinate circadian oscillators in the forebrain as well as to assess the potential for circadian plasticity in the limbic forebrain, experiments in the present thesis were done to assess locomotor activity rhythms and PER2 expression in the SCN and several limbic forebrain structures in rats housed under a 26-h LD condition for different durations. A brief account of photic resetting and entrainment of circadian rhythms pertinent to this thesis are given below.

Circadian Rhythms

Circadian rhythms are 24-h fluctuations in behavioral and physiological functions that evolved in response to the need to adapt to the 24-h day/night cycle. For example, circadian rhythms are seen in the sleep/wake cycle, mood, feeding, body temperature, heart rate, hormone secretion, and gene expression (Cassone, Warren, Brooks, & Lu, 1993). In mammals, these rhythms are endogenous and are controlled by a network of oscillators that are synchronized by a master circadian clock located in the SCN of the hypothalamus (Lowrey & Takahashi, 2000). The master clock is appropriately named, in that lesions of the SCN (SCNX) induce complete behavioral and physiological arrhythmicity (Stephan & Zucker, 1972), while fetal SCN transplants restore locomotor rhythmicity in SCN-ablated recipients with the period of the donor (Lehman et al., 1987; Ralph, Foster, Davis, & Menaker, 1990).

It is believed that most, if not all, of the ~20 000 cells in the SCN are self-sustained autonomous oscillators (Welsh, Logothetis, Meister, & Reppert, 1995). At the cellular level, the generation of circadian rhythms is made possible via an intricate

interplay between a small set of core clock genes that make up the circadian molecular clock. The molecular clock is comprised of transcription/translation auto-regulatory feedback loops consisting of positive elements, BMAL1 and CLOCK, and negative elements, the *Period* (*Per1*, *Per2*, *Per3*) and *Cryptochrome* (*Cry1*, *Cry2*) genes (Ko & Takahashi, 2006; Okamura, Yamaguchi, & Yagita, 2002). Specifically, CLOCK and BMAL1 activate the transcription of the *Per* and *Cry* genes, and the resulting protein products, in turn, feedback and inhibit the transcriptional activation of CLOCK and BMAL1. This process takes ~24hrs to complete and is thought to underlie the 24-h rhythmicity seen in physiology and behavior. *Period2* and its protein product PER2 have been shown to be a critical component of the molecular clock (Bae et al., 2001; Zheng et al., 1999) and its level of expression has been used as a marker for circadian oscillators in the brain and periphery (Amir, Lamont, Robinson, & Stewart, 2004; Yoo et al., 2004).

Entrainment

In the absence of timing cues, behavioral outputs of the master clock, such as locomotor activity, reveal an endogenous "free running" rhythm that is slightly different from 24hrs. Thus, the SCN is not only responsible for the generation of rhythms, but also for entrainment to the LD cycle. Light is the major environmental synchronizer, or *zeitgeber* (time giver), that entrains the SCN on a daily basis (Rusak & Zucker, 1979). Light is communicated to the SCN directly from the retina via the retinohypothalamic tract (RHT) (Moore & Lenn, 1972) and causes the SCN to make daily adjustments to coincide with the 24-h LD cycle. The response of the SCN clock to light varies according to the phase of the circadian cycle. Light presented during the day (or subjective day) has no effect on circadian rhythms, whereas light presented during the night (or subjective

night) causes phase shifts. Specifically, light presented early in the night causes phase delays, and light presented in the late night causes phase advances. Knowledge about the differential sensitivity of the SCN to light allows experimental manipulation of the LD cycle such that the period of the entraining cycle can be manipulated and the non-specific (masking) effects of light minimized. A T-cycle (one light pulse per cycle) is one such tool that has been used in the study of entrainment. Using a T-cycle shorter that an organism's free-running period will lead to entrainment by phase advances, and using a T-cycle longer than the free-running period will lead to entrainment by phase delays. However, the period of the T-cycle can be outside of the capabilities of the circadian clock to entrain, such that 21-h or 27-h T-cycles fail to lead to stable entrainment whereas 23-h and 26-h T-cycles are effective (Stephan, 1983).

Extra-SCN oscillators

Although the SCN is considered the master pacemaker, in recent years, circadian oscillators have been found throughout the mammalian brain (Abe et al., 2002; Amir, Lamont, Robinson, & Stewart, 2004; Lamont, Robinson, Stewart, & Amir, 2005) and in peripheral organs and tissues, including the lung, heart, and liver (Hogenesch, Panda, Kay, & Takahashi, 2003; Yamazaki et al., 2000). The SCN is thought to act as a conductor, synchronizing rhythms in subordinate oscillators throughout the brain and periphery (Yoo et al., 2004).

Yamazaki et al (2000) have shown circadian rhythms in rat peripheral tissues using *Per1-luciferase* transgenic rats. Cultured explants of the liver, lung, and skeletal muscle continued to oscillate for two to seven days without input from the SCN before damping out. Furthermore, this damping was not due to cell death, as rhythmicity was

reinstated with medium change. It seems that without input from the SCN, rhythms in peripheral tissue remain synchronized for short periods of time before becoming uncoupled.

Also using the *Per1-luciferase* transgene as a marker for circadian oscillations, Abe and colleagues (2002) found that although many structures in the brain exhibit some rhythms *in vitro*, only four structures besides the SCN, the olfactory bulbs, the arcuate nucleus, and the pineal and pituitary glands, showed near 24-h oscillations and continued to do so for more than 3 cycles before damping out.

Subordinate oscillators in the limbic forebrain

Using immunocytochemistry for the clock protein PER2, Amir and colleagues have found subordinate circadian oscillators in several limbic forebrain areas that are known to be involved in emotion, motivation, and memory; the BNSTov, the central nucleus of the amygdala (CEA), the basolateral amygdala (BLA) and the dentate gyrus (DG) of the hippocampus (Amir, Lamont, Robinson, & Stewart, 2004; Lamont, Robinson, Stewart, & Amir, 2005). The BNSTov and CEA are two regions that are highly anatomically interconnected, and neurochemically and functionally related (Day, Curran, Watson, & Akil, 1999; Swanson, 2003). Together, these regions are commonly referred to as the central extended amygdala, and have been shown to be involved in multiple behavioral systems including: feeding (Petrovich & Gallagher, 2003); drug addiction and relapse (Day et al., 2001; Erb, Salmaso, Rodaros, & Stewart, 2001; Erb, Shaham, & Stewart, 2001); and fear and anxiety (Davis, 1998; Lee & Davis, 1997). The BLA resembles the neighboring cortex more than the rest of the amygdala, and mainly projects to the CEA and other regions in the amygdala, the cortex, and the hippocampus

through the entorhinal cortex (Dong, Petrovich, & Swanson, 2001; Dong, Petrovich, Watts, & Swanson, 2001; Petrovich, Canteras, & Swanson, 2001), but does not have dense connections to the BNSTov (Dong, Petrovich, & Swanson, 2001). The hippocampus sends extensive projections to most of the amygdala (Petrovich, Canteras, & Swanson, 2001). Together, the hippocampus and amygdala are thought to play an important role in the integration of learning and memory of emotional states.

Studies of the nature of the expression of PER2 in these limbic areas revealed two basic patterns: the BNSTov and CEA are synchronized and in phase with the SCN showing peak PER2 expression in the early evening (activity onset for nocturnal rodents), while the DG and BLA are synchronized but 180° out of phase with the SCN, with peak expression in the early morning (activity offset for nocturnal rodents) (Amir, Lamont, Robinson, & Stewart, 2004; Lamont, Robinson, Stewart, & Amir, 2005).

Studies of the mechanisms that control the rhythms of PER2 expression in these limbic forebrain areas have shown that they are all under the control of the SCN. SCNX completely blunt PER2 rhythms in these regions (Lamont, Diaz, Barry-Shaw, Stewart, & Amir, 2005) and unilateral SCNX blunt rhythmic PER2 expression in the BNSTov ipsilateral to the lesioned SCN, suggesting that the rhythm in PER2 expression observed in the BNSTov is due, in part, to ipsilateral neural connections from the SCN (Amir, Lamont, Robinson, & Stewart, 2004). Bilateral adrenalectomy was also found to blunt PER2 rhythms in the BNSTov and CEA, but not in BLA and DG (Amir, Lamont, Robinson, & Stewart, 2004; Segall, Perrin, Walker, Stewart, & Amir, 2006) and this effect was reversed by corticosterone administration in the drinking water but not via a constant release pellet (Segall, Perrin, Walker, Stewart, & Amir, 2006). These data

suggest that the PER2 rhythm in the BNSTov and CEA depend on the rhythm rather than the mere presence of corticosterone in the circulation. Finally, it was found that the rhythms of PER2 expression in the limbic forebrain are sensitive to treatments that disrupt energy balance. Specifically, daily restricted feeding schedules which are known to induce food anticipatory behavioral and physiological rhythms, including body temperature and corticosterone secretion (Boulos & Terman, 1980; Mistlberger, 1994; Stephan, 2002), can entrain the PER2 rhythms in the BNSTov, CEA, BLA and DG and uncouple them from the SCN (Lamont, Diaz, Barry-Shaw, Stewart, & Amir, 2005; Waddington Lamont et al., 2007).

Weak coupling between the master clock and subordinate oscillators

It has been shown that large shifts in the LD cycle disrupt the phase relationship between the SCN and subordinate clocks throughout the body. Yamazaki and colleagues (2002) imposed either 6-h phase advances or delays on *Per1-luciferase* transgenic rats and compared rhythms in *Per1* bioluminescence in peripheral tissues with those in the SCN. In both the phase advance and delay groups, the rhythm of *Per1* expression in the SCN was able to shift almost completely after the first day, whereas *Per1* rhythms in liver, lung, and skeletal muscle took significantly longer before completely adjusting to the phase shift, with phase advances proving more slow than phase delays. Similar results were found in the brain. Abe and colleagues (2002) showed that after 6-h phase advances or delays, the arcuate nucleus, paraventricular nucleus, and pineal gland took longer than the SCN to adjust to the phase shift and show expected levels of *Per1* expression and peaks. Finally, Amir and colleagues (2004) showed that an 8-h delay or advance in the LD cycle caused PER2 expression in the BSNTov to lag behind the SCN by several days

before reaching normal levels. Together, the findings that large shifts in the entraining light cycle are associated with differential rates of re-entrainment of clock gene rhythms in the SCN compared with those in other areas, suggest the existence of weak coupling between the master clock and subordinate oscillators in the brain and periphery.

Objective

The studies in the present thesis were undertaken to further investigate the nature of the coupling between the SCN clock and subordinate oscillators in the limbic forebrain. Previous work has shown that a single large shift in the entraining light cycle led to differential rates of re-entrainment of PER2 expression between the SCN and BNSTov. However, the effect of daily (chronic) small shifts on the entrainment of subordinate oscillators has not been investigated. Behavioral rhythms and the expression of PER2 in the SCN are readily entrained by light cycles longer or shorter than the normal 24-h light cycle. Here I examined the effect of exposure to a 26-h T-cycle (T26; 1-h:25-h LD) compared to a 24-h T-cycle (T24, 1-h:23-h LD) on the expression of the clock protein PER2 in the SCN and four regions of the limbic forebrain known to exhibit circadian oscillations in PER2 expression, the BNSTov, CEA, BLA, and DG. Based on previous work on the expression of PER2 in the SCN carried out in our laboratory (Beaule, Houle, & Amir, 2003) it was expected that the SCN would entrain readily to both T24 and T26 cycles and show no differences in the pattern of PER2 expression. The effect of entrainment to a long T-cycle on PER2 rhythms in the limbic forebrain could not be predicted a priori. However, it was expected that the rhythm in PER2 expression in the BNSTov and CEA would mirror each other.

In experiment 1 the effect of a 26-h T-cycle on PER2 expression in the SCN and limbic forebrain regions was investigated using rats maintained on a T-cycle schedule for 7, 14, 30, or 60 days, and sacrificed at one of 2 time points: activity onset or offset.

Experiment 2 was done to examine with more precision the effect of prolonged exposure to a T26 cycle on the circadian rhythm of PER2 expression in the SCN and limbic forebrain regions. To do this, rats were maintained on a T-cycle for 30 days and sacrificed at one of 4 time points; activity onset, onset +7hrs, offset, or offset +7hrs.

METHODS

Animals and Housing

Adult male Wistar rats (weighing approximately 200 grams at the start of experiments; Charles River St-Constant, QC, Canada) were used in these experiments. Rats were individually housed in plastic cages equipped with running wheels at an ambient temperature and had *ad libitum* access to rat chow and water. Each cage was isolated within a ventilated, sound and light-tight chamber equipped with a computer-controlled lighting system (VitalView; Mini Mitter Co. Inc., Sunriver, OR, USA). Each running wheel was equipped with a magnetic microswitch connected to a computer. Running-wheel activity was recorded continuously and displayed in 10-min bins using VitalView software. Using Circadia software, double plotted actograms were created to display and analyze running-wheel activity rhythms at each stage of the experiments. All procedures were carried out in accordance with the Canadian Council on Animal Care guidelines and were approved by the Animal Care Committee of Concordia University.

Procedure

To facilitate entrainment to the T-cycles, rats were first entrained to a 12-h:12-h LD cycle (light = 300 lux at cage level) for approximately 2 weeks, and then placed under either a 1-h:23-h LD cycle (24h T-cycle) or a 1-h:25-h LD cycle (26h T-cycle), for 7, 14, 30, or 60 days. For all rats, the onset of the first 1-h light pulse corresponded to light onset of the established LD cycle, and this time of light presentation was maintained for the T24 group. For rats in the T26 condition, each subsequent daily light pulse was delayed by 2 hours to correspond to a 26-hour day.

Tissue Preparation

At the appropriate time and day, rats were deeply anesthetized with sodium pentobarbital (~100mg/kg, *i.p.*) prior to transcardial perfusion with 300ml of cold saline (0.9% NaCl), followed by 300ml of cold paraformaldehyde (4% in a 1M phosphate buffer, pH 7.3). Whole brains were removed and post-fixed overnight in paraformaldehyde at 4°C. Serial coronal sections (50μm thick) through regions of interest were collected using a Vibratome (St-Louis, MO, USA) and stored in Watson's Cryoprotectant at –20°C until processed for immunocytochemistry.

Immunocytochemistry

Free-floating sections were rinsed (6X 10 min) in cold 0.9% Trizma buffered saline (TBS; pH 7.6) and incubated in a hydrogen peroxide quench solution (3% H_2O_2 in TBS) for 30 min at room temperature (RT). Sections were then rinsed (3X 10 min) in TBS and incubated in a pre-block solution made of 0.3% Triton X-100 in TBS (Triton-TBS) and 5% Normal Goat Serum (NGS), for one hour at 4°C, and then directly transferred into the primary solution. Sections were incubated in PER2 polyclonal

antibody raised in rabbit (Alpha Diagnostic International, San Antonio, TX, USA) diluted 1:800 in Triton-TBS and 3% NGS, and incubated for approximately 48hrs at 4°C. After the primary antibody incubation, sections were once again rinsed in cold TBS and then transferred to a secondary solution consisting of biotinylated anti-rabbit IgG made in goat (Vector Laboratories, Burlington, ON, Canada) diluted 1:200 in Triton-TBS and 3% NGS for one hour at 4°C. After incubation with the secondary antibody, sections were rinsed (3X 10 min) with cold TBS and incubated in a tertiary solution (avidin biotin peroxidase complex in TBS) for 2hrs at 4°C (Vectastain Elite ABC Kit, Vector Laboratories). Finally, sections were rinsed in TBS, and then again in cold 50 mM Tris-HCl for 10 min. Sections were then incubated for 10 min in 0.05% 3,3´-diaminobenzidine (DAB) in Tris-HCl and further incubated for 10 min in a DAB/50 mM Tris-HCl with 0.01% H_2O_2 and 8% $NiCl_2$. Sections were rinsed a final time in cold TBS and wet-mounted onto gel-coated microscope slides, allowed to dry overnight, and then dehydrated through graded ethanol concentrations, soaked in Citrisolve (Fisher Scientific, Houston, TX, USA) for a minimum of 30 min, and finally cover-slipped with Permount (Fisher).

Data Analysis

Behavior

Actograms were visually analyzed for entrainment throughout the experiments. To determine when activity onset or offset would occur on the day of perfusion, a line of best fit was drawn at activity onset or offset using the ~7 days of activity prior to the perfusion day. To determine the period of each rat at the end of the experiments, a line of best fit was drawn at activity onset using the last ~7-10 days of behavior.

Brain

Brain sections containing the BNSTov, SCN, BLA, CEA, and DG were examined under a light microscope (Leitz Laborlux S), and digitized using a Sony XC-77 Video Camera connected to a Scion LG-3 frame grabber using NIH Image software (v1.63). Multiple bilateral images from the SCN, BNSTov, CEA and BLA were captured using a 400X400 μm template, and a 200X400 μm template was used for the DG. Cells immunopositive for PER2 were counted by an observer blind to group membership using Image SXM software (v1.79). An average of the 5 sections containing the highest number of labeled nuclei for each region was calculated for each subject.

Experiment 1

To determine the time course of any effects of the manipulation on PER2 expression in brain regions of interest, rats in both the T24 and T26 conditions were perfused after varying lengths of exposure to the T-cycle: 7 days; 14 days; 30 days; or 60 days. In addition, to examine the interaction between the effects of the T-cycle schedule and time of day, half of the rats perfused on each day were sacrificed at activity onset (ON), and the other half at activity offset (OFF). The precise time points were arrived at by examining each rat's actograms the day before perfusion.

The time course of the effects of the T-cycle manipulation on PER2 immunoreactivity in the BNSTov, SCN, BLA, CEA, and DG were-examined using a 3-way analysis of variance (ANOVA), with T-cycle (T24/T26), perfusion time (ON/OFF), and day of perfusion (D17, D14, D30, and D60) as the independent variables. Significant interactions were further investigated using a 2-way ANOVA at each Day and t-tests

where appropriate. The alpha level was set at 0.05 for all analyses. N equals 4 for all groups in this experiment.

Experiment 2

To examine in more detail the temporal changes in PER2 expression seen in rats housed under a 26-h T-cycle, in Experiment 2, rats were kept on either a T24 or T26 schedule for 30 days, and were sacrificed at one of 4 time points based on running-wheel behavior: activity onset, onset +7hrs, activity offset, or offset +7hrs.

The effects of the T-cycle manipulation on PER2 immunoreactivity in the BNSTov, SCN, BLA, CEA, and DG were examined using 2-way ANOVAs with T-cycle (T24/T26) and time of perfusion (ON, ON +7hrs, OFF, or OFF +7hrs) as the independent variables. Significant interactions were further investigated using tests for simple main effects and, where appropriate, pairwise comparisons. The alpha level was set at 0.05 for all analyses. N equals 4 for all groups in this experiment, except for T24 ON +7hrs (N=3), and T26 ON +7hrs and OFF +7hrs (N=5).

RESULTS

Experiment 1: Across Days

Behavior

In the initial phase of the experiment, when all rats were exposed to a 12-h:12-h LD schedule, the majority of their locomotor activity was restricted to the dark phase of the cycle and hence they were considered to be entrained. Furthermore, all rats gradually adjusted to their given T-cycle, with this adjustment being slower for T26 rats. The average period (in hrs) for T24 and T26 rats at each of the different days was as follows,

T24: D7=24 ±0.01, D14=23.94 ±0.03, D30=23.99 ±0.01, D60=23.99 ±0.01; T26: D7=24.09 ±0.03, D14=25.14 ±0.08, D30=26.04 ±0.03, D60=26 ±0.02. Figure 1 shows representative double-plotted actograms for T24 rats on a T-cycle for 60 days. As can be seen by this figure, rats remained entrained to the 24-h cycle. Figure 2 shows representative double-plotted actograms for T26 rats on a T-cycle for 60 days. As can be seen by this figure, rats that were sacrificed after 7 days on a T26 schedule were unaffected by the T-cycle because the light pulse fell during a time known not to have any effect on behavior, the subjective day of the rat (Pittendrigh & Daan, 1976). However, once the light pulse reached activity onset, which marks the beginning of the light sensitive region and occurred on ~day 7-9, rats began to entrain to the T26 cycle by producing daily phase delays. As can be seen by the scatterplot graphs in Appendix A, the amount of wheel-running behavior during the active phase varied considerably between rats. However, there were no significant differences in the number of hours from activity onset to offset between T24 and T26 rats sacrificed at activity offset, with rats on a T24 cycle running on average 9.53 hrs ±0.32 and rats on a T26 cycle running on average 10.36 hrs ±0.52.

PER2 Immunoreactivity

SCN

Figure 3 shows representative photomicrographs of the SCN for both T-cycle groups at activity onset on each of Days 7, 14, 30 and 60, and Figure 4 shows mean PER2-immunoreactivity (PER2-ir) for the same groups at both activity onset and offset on each of the Days. As these figures show, there was little change in the pattern of PER2-ir in the SCN across days or between groups. Analyses of these data showed that

overall PER2-ir was higher at activity onset than offset (significant effect of perfusion time, $F_{(1,48)}$= 575.927, p<.0001). None of the other main effects or interactions reached significance, with the exception of a significant 2-way interaction between perfusion time and day (Perfusion time X Day, $F_{(3,48)}$= 2.912, p<.05). This latter interaction is reflected in the differences in the amount of PER2-ir between days and may just be a consequence of variability between immunocytochemistry runs on levels of PER2 expression.

BNSTov

Figure 5 shows representative photomicrographs of the BNSTov for both T-cycle groups at activity onset on each of Days 7, 14, 30 and 60, and Figure 6 shows mean PER2-ir for the same groups at both activity onset and offset on each of the Days. As Figure 6 demonstrates, there were effects of T-cycle on the pattern of PER2 expression in this brain region that developed across time such that there was a reduction in PER2-ir at activity onset in the T26 group on Days 30 and 60, resulting in what appears to be a blunting of the rhythm.

These changes were reflected in the results of the analyses of these data, which showed significant main effects of T-cycle, $F_{(1,48)}$= 8.337, p<.01, perfusion time, $F_{(1,48)}$= 101.020, p<.0001, and Day, $F_{(3,48)}$= 2.825, p<.05. These significant main effects were modified by a significant 3-way interaction among these variables ($F_{(3,48)}$= 3.508, p<.05). To investigate these effects further, 2-way ANOVA were performed on data from each testing day. Consistent with Figure 6 panels A and B, analysis of the data for Day 7 and Day 14 showed only a significant increase in PER2-ir at activity onset (main effect of perfusion time: D7, $F_{(1,12)}$= 39.707, p<.0001; D14, $F_{(1,12)}$= 46.606, p<.0001).

As Figure 6 panels C and D show, there was a reduction in PER2-ir at activity onset on Days 30 and 60. This effect was reflected in significant main effects of T-cycle, D30, $F_{(1,12)}$= 8.225, p<.05, and perfusion time, D30, $F_{(1,12)}$= 9.701, p<.01; D60, $F_{(1,12)}$= 15.440, p<.005, which were modified by significant interactions between T-cycle and perfusion time on both testing days (D30, $F_{(1,12)}$= 36.196, p<.0001; D60, $F_{(1,12)}$= 12.651, p<.005). Post-hoc analyses showed that PER2-ir was higher in the T24 group than the T26 group at activity onset for both Day 30 and 60 (ON: D30, $t_{(6)}$= 6.249, p<.001; D60, $t_{(6)}$= 3.891, p<.01) but that the groups did not differ significantly at activity offset.

CEA

Figure 7 shows representative photomicrographs of the CEA for both T-cycle groups at activity onset on each of Days 7, 14, 30 and 60, and Figure 8 shows mean PER2-ir for the same groups at both activity onset and offset on each of the Days. As Figure 8 shows, the pattern of PER2-ir in the CEA was very similar to that in the BNSTov, such that PER2 expression was reduced at activity onset in the T26 group at both days 30 and 60 resulting in what appears to be a blunting of the rhythm. A 3-way ANOVA performed on these data showed significant main effects of T-cycle, $F_{(1,48)}$= 4.264, p<.05, and perfusion time, $F_{(1,48)}$= 44.899, p<.0001. The 3-way interaction showed a trend towards significance ($F_{(3,48)}$= 2.632, p=.0606).

To investigate these effects further, 2-way ANOVA were performed on data from each testing Day. Analysis of the data for Day 7 and Day 14 showed main effects of perfusion time, D7 $F_{(1,12)}$= 12.740, p<.005: D14 $F_{(1,12)}$= 129.946, p<.0001. On Day 14 there was also a significant interaction between T-cycle and perfusion time ($F_{(1,12)}$= 5.943, p<.05), and pairwise comparisons showed that PER2-ir was higher in the T26 group than

in the T24 group at activity offset (OFF, $t_{(6)}$= -3.955, p<.01) but that there was no significant difference between the groups at activity onset.

Analyses of the data for D30 and Day 60 revealed a significant main effect of T-cycle at Day 30 ($F_{(1,12)}$= 4.865, p<.05), a significant main effect of perfusion time at Day 60 ($F_{(1,12)}$= 8.595, p<.05) and a significant interaction between T-cycle and perfusion time at both days (D30, $F_{(1,12)}$= 13.343, p<.005; D60, $F_{(1,12)}$= 15.580, p<.005). Post-hoc pairwise comparisons showed higher PER2-ir in the T24 group compared to the T26 group at activity onset for both Day 30 and 60 (ON: D30, $t_{(6)}$= 4.231, p<.01; D60, $t_{(6)}$= 3.802, p<.01) and no significant difference at activity offset.

BLA

Figure 9 shows representative photomicrographs of the BLA for both T-cycle groups at activity offset on each of Days 7, 14, 30 and 60, and Figure 10 shows mean PER2-ir for the same groups at both activity onset and offset on each of the Days. Analyses of these data showed that overall PER2-ir was higher at activity offset than activity onset (significant main effect of perfusion time, $F_{(1,48)}$= 128.585, p<.0001). None of the other main or interaction effects reached significance.

DG

Figure 11 shows representative photomicrographs of the DG for both T-cycle groups at activity offset on each of Days 7, 14, 30 and 60, and Figure 12 shows mean PER2-ir for the same groups at both activity onset and offset on each of these days. Analyses of these data showed that, like the BLA, overall PER2-ir was higher at activity offset than onset (significant main effect of perfusion time, $F_{(1,48)}$= 225.574, p<.0001). None of the other main or interaction effects reached significance with the exception of a significant 2-way

interaction between perfusion time and Day ($F_{(3,48)}$= 5.461, p<.005). This latter interaction is reflected in the differences in the amount of PER2-ir between days and may just be a consequence of variability between immunocytochemistry runs on levels of PER2 expression.

Experiment 2: Across Hours

Behavior

As in Experiment 1, all rats entrained to the initial 12-h:12-h LD schedule, and adjusted to their given T-cycle. The average period for T24 rats was 23.94±0.01 and for T26 rats was 26.01±0.02. Figure 13 shows representative double-plotted actograms for T24 and T26 rats 30 days on a T-cycle. Consistent with Experiment 1, for the first week on the T26 schedule, rats were unaffected by the light pulse given that it fell during the subjective day. Once the light pulse reached activity onset, at ~Day 7-9, rats began to entrain to the T26 cycle by producing daily phase delays (see Figure 13B).

PER2 Immunoreactivity

SCN

Figure 14 shows representative photomicrographs of the SCN for both T24 and T26 groups at activity onset, and mean PER2-ir in the SCN for both groups across 4 perfusion times at Day 30. As can be seen by Figure 14B, levels of PER2-ir change across the sample times (significant main effect of perfusion time, $F_{(3,25)}$= 75.720, p<.0001). Post hoc pairwise comparisons showed that PER2 expression was highest at activity onset and lowest at activity offset. Neither the main effect of T-cycle nor the interaction effect were significant (T-cycle, $F_{(3,25)}$= .240, p>.05; interaction, $F_{(3,25)}$= 1.109, p>.05).

BNSTov

Figure 15 shows representative photomicrographs of the BNSTov for both T24 and T26 groups at activity onset, and mean PER2-ir in the BNSTov for both groups across the 4 perfusion times at Day 30. As can be seen by Figure 15B, there was an effect of T-cycle on the pattern of PER2-ir across the sample times such that the rhythm in PER2 expression in the T26 group was shifted. These effects were reflected in significant main effects of perfusion time ($F_{(3,25)}$= 17.342, p<.0001) and interaction ($F_{(3,25)}$= 11.198, p<.0001), but not in group (T-cycle, $F_{(3,25)}$= 2.991, p>.05). This interaction was investigated by conducting simple main effects analyses on the data for the T24 and T26 groups across perfusion times. Analyses of both the T24 and T26 group revealed significant effects of perfusion time, $F_{(3,14)}$ =17.792, p<.001and $F_{(3,14)}$ =13.254, p<.001, respectively. Post-hoc analyses revealed highest amounts of PER2-ir at activity onset and offset +7hrs in the T24 group, and a trend towards significance at activity offset +7hrs (p= 0.06) in the T26 group. The lowest amounts of PER-ir were found at activity offset and onset +7hrs in the T24 group and at activity onset +7hrs for the T26 group.

CEA

Figure 16 shows representative photomicrographs of the CEA for both T24 and T26 groups at activity onset, and mean PER2-ir in the CEA for both groups across 4 perfusion times at Day 30. Like the BNSTov, PER2-ir in the CEA was affected by T-cycle across sample times such that the rhythm of PER2 expression in the T26 group was shifted. These effects were reflected in significant main effects of perfusion time ($F_{(3,25)}$= 13.041, p<.0001) and interaction ($F_{(3,25)}$= 10.938, p<.0001), but not in group (T-cycle, $F_{(3,25)}$= 2.672, p>.05). This interaction was investigated by conducting simple main effects

analyses on the data for the T24 and T26 groups across perfusion times. Analyses of both the T24 and T26 group revealed significant effects of perfusion time, $F_{(3,11)}$=27.314, p<.0001 and $F_{(3,14)}$=9.828, p<.001, respectively. Post-hoc analyses showed highest amounts of PER2-ir at activity onset for the T24 group and at activity offset +7hrs and activity offset for the T26 group. Lowest amounts of PER2-ir were found at activity offset in the T24 group and at activity onset +7hrs in the T26 group.

BLA

Figure 17 shows mean PER2-ir in the BLA for both T24 and T26 groups across 4 perfusion times at Day 30. As can be seen by this figure, levels of PER2-ir change across the sample times (significant effect of perfusion time, $F_{(3,25)}$= 5.724, p<.005) and group (significant main effect of T-cycle, $F_{(3,25)}$= 4.087, p≤.05). Post hoc pairwise comparisons showed that PER2 expression was highest at activity offset and onset +7hrs and lowest at activity onset and offset +7hrs. Furthermore, overall, PER2 expression in the T26 rats was elevated compared to that in T24 rats. The interaction effect failed to reach significance ($F_{(3,25)}$= .784, p>.05).

DG

Figure 18 shows mean PER2-ir in the DG for both T24 and T26 groups across 4 perfusion times at Day 30. Unlike the BLA, PER2-ir in the DG was affected by T-cycle across the sample times. These effects were reflected in significant main effects of perfusion time ($F_{(3,25)}$= 42.348, p<.0001) and interaction ($F_{(3,25)}$= 5.241, p<.01), but not in T-cycle group ($F_{(1,25)}$= .408, p>.05). This interaction was investigated by conducting simple main effects analyses on the data for the T24 and T26 groups across perfusion times. Analyses of both T24 and T26 groups revealed significant effects of perfusion

time, $F_{(3,11)}$ =33.605, p<.0001 and $F_{(3,14)}$ =17.686, p<.0001, respectively. Post-hoc analyses showed highest levels of PER2-ir at activity offset and activity onset +7hrs for the T24 group, and at activity offset +7hrs for the T26 group. Lowest amounts of PER2-ir were found at activity onset and offset +7hrs for the T24 group, and at activity onset, activity offset and activity offset +7hrs for the T26 group.

ANOVA tables for both experiments can be seen in Appendix B.

DISCUSSION

The present thesis sought to examine the strength of the coupling between the master clock and subordinate oscillators in the limbic forebrain by comparing the rhythms of expression of PER2 in the SCN, BNSTov, CEA, BLA and DG in rats housed under normal (24-h LD cycle) and extreme (26-h LD cycle) entrainment conditions. It was found that prolonged exposure to a 26-h T-cycle uncoupled the rhythms and led to the establishment of a new phase relationship between the rhythms in the BNSTov and CEA and those in the SCN, BLA and DG, and, in addition, changed the level of PER2 expression in the two latter structures. These results demonstrate that the strength of the coupling between the SCN clock and subordinate oscillators in the limbic forebrain vary from one structure to another.

As expected, locomotor activity rhythms and PER2 expression in the SCN stably entrained to the extended 26-h period, with PER2 levels peaking at activity onset for rats in all groups. Unlike the effects of acute large phase shifts in the 24-h day previously described (Abe et al., 2002; Amir, Lamont, Robinson, & Stewart, 2004), it seems that the

SCN is able to adapt to this 26-h lighting schedule, in which chronic daily phase delays are required.

The results from Experiment 1 reveal that levels of PER2-ir in the BNSTov and CEA were significantly altered at activity onset after 30 and 60 days on a T26 cycle, suggesting the possibility that the PER2 rhythms in these regions were blunted. Whereas, the expression of PER2-ir in the BLA and DG was unaffected by the T26 cycle at the two time points examined in this experiment.

Given that for the first ~7 days the T-cycle light pulse in the T26 schedule fell at a time when light has been shown to have no effect on activity (Pittendrigh & Daan, 1976), rats in the T26 Day 7 group can be thought of as a control. The fact that the PER2 expression in the T26 Day 7 group resembled that of rats under normal (T24) entrainment conditions supports this interpretation. The results from Day 14 indicate that the phase relationship between the SCN and oscillators in the limbic forebrain are able to withstand the shift to a 26-h schedule for about a week; the findings concerning PER2 expression from this group are similar to those killed at Day 7 (0 days on an effective T-cycle).

Importantly, the findings from Experiment 1 show that in rats housed under a 26-h T-cycle, the expression of PER2-ir in the central extended amygdala becomes different from that in the SCN as the number of days on the T-cycle increases. This finding is confirmed in Experiment 2 at day 30, and adds to these results by showing that indeed the rhythm in the BNSTov and CEA is not absent, but instead is uncoupled from the SCN and is dampened at the usual peaking time (activity onset). Although this study revealed a significant effect of T-cycle group in the BLA and interaction effect between T-cycle group and perfusion time in the DG, the pattern of the PER2 rhythm in T24 and T26

groups remained similar and only the level of expression was altered at certain time points.

The results of the present study demonstrate that in rats housed under a 26-h T-cycle, the rhythm of PER2 expression within specific limbic forebrain areas becomes uncoupled from that of the SCN somewhere between 8 and 23 days after the onset of entrainment. Furthermore, once the new phase relationship between the SCN rhythm and the rhythm in the BNSTov and CEA has been established, it appears to remain stable.

The cause of the uncoupling of the rhythms of the BNSTov and CEA from that in the SCN is unknown and cannot be determined by the present experiments. One possibility is that the change in the phase of the PER2 rhythm in the BNSTov and CEA observed under the T26 cycle is linked to a change in the rhythm or level of circulating corticosterone (CORT) brought about by the long entraining light cycle. Previous studies from our laboratory have shown that the rhythm of PER2 expression in the BNSTov and CEA depends on intact CORT rhythms (Amir, Lamont, Robinson, & Stewart, 2004; Segall, Perrin, Walker, Stewart, & Amir, 2006). However, preliminary results from our laboratory comparing CORT levels in T24 and T26 rats have shown no differences between the two groups (see Appendix C). This suggests that CORT is not the cause of the disrupted PER2 rhythms in the central extended amygdala.

Daily changes in feeding time imposed by housing under a T26 schedule could also contribute to the change in PER2 expression in the BNSTov and CEA. We have shown previously that the rhythm of PER2 in the BNSTov and CEA is sensitive to nutritional status and can be uncoupled from the SCN rhythm by scheduled feeding (Lamont, Diaz, Barry-Shaw, Stewart, & Amir, 2005; Waddington Lamont et al., 2007).

However, scheduled feeding has also been found to affect the PER2 rhythms in the BLA and DG (Waddington Lamont et al., 2007). Given that prolonged housing under T26 did not result in uncoupling of the PER2 rhythm in the BLA and DG from the SCN rhythm, a role for feeding in the uncoupling of the BNSTov and CEA rhythm is unlikely.

The pineal hormone, melatonin, has been shown to entrain circadian behavioral rhythms and to play a key role in the regulation of the expression of clock genes in some brain regions in rodents (Jilg et al., 2005; Uz, Akhisaroglu, Ahmed, & Manev, 2003; von Gall et al., 2002). The release of melatonin from the pineal is highly sensitive to light and it is likely that in the present study the rhythm of circulating melatonin was strongly affected by the daily change in the time of light exposure associated with housing under T26. Furthermore, the BNST, amygdala and hippocampus have all been shown to contain melatonin binding sites (Laudon, Nir, & Zisapel, 1988; Musshoff, Riewenherm, Berger, Fauteck, & Speckmann, 2002). Thus it is possible that the change in PER2 rhythms induced by housing under T26 may be linked to the daily changes in the melatonin rhythm associated with entrainment to the T26 cycle. We have found, however, that surgical removal of the pineal gland has no effect on the rhythm of PER2 expression in these regions (Amir, Harbour, & Robinson, 2006), a finding that argues against a role for melatonin in the uncoupling of the BNSTov and CEA PER2 rhythm from the rhythm of the SCN.

The BNSTov and CEA are known to play important roles in motivational and emotional regulation. Therefore, it is highly probable that circadian disruption in these areas induced by prolonged exposure to a 26-h LD cycle would have notable behavioral and physiological consequences. Future studies will be needed to determine exactly what

these consequences may be. Interestingly, it has been shown recently that housing under a 26-h T-cycle blocks behavioral sensitization and conditioned place preference to cocaine in rats (Renteria Diaz & Arvanitogiannis, 2005; Renteria Diaz & Arvanitogiannis, 2006). However, a link between the disruption of cocaine-related responses and changes in the rhythm of expression of PER2 in the central extended amygdala has not been explored.

More work is needed in order to establish the functional impact of the changes in phase relationship between the SCN and subordinate oscillators in the central extended amygdala. It is believed that one of the key roles of subordinate oscillators in the brain is to maintain the operational integrity of neural circuits by regulating basic processes at the cell and tissue levels (Tu & McKnight, 2006). Accordingly, changes in the timing of such processes within the central extended amygdala may affect communication between this and other behaviorally important networks and, ultimately, alter the way in which motivationally and emotionally significant stimuli are translated into appropriate behavioral and physiological responses. In humans, appropriate alignment of central and peripheral circadian oscillations is thought to be critical for the proper temporal organization of physiology and behavior; disruptions in circadian rhythms have been implicated in sleep disorders, cognitive dysfunction, mood disorders, and general malaise as seen in jet lag and shift workers (Bunney & Bunney, 2000). A greater understanding of the relationship between the various circadian oscillators in the brain and periphery is critical for better diagnosis and treatment of desynchronization disorders.

In conclusion, the present work shows that entrainment to long light cycles shift the PER2 rhythm of the BNSTov and CEA without affecting PER2 rhythms in the SCN

and entrainment of circadian locomotor behavior. These findings are consistent with the idea that the coupling between the SCN clock and subordinate oscillators in the central extended amygdala is weak and vulnerable to significant changes in the environmental light cycle. The functional consequences of this tissue-specific vulnerability are presently under investigation.

FIGURES

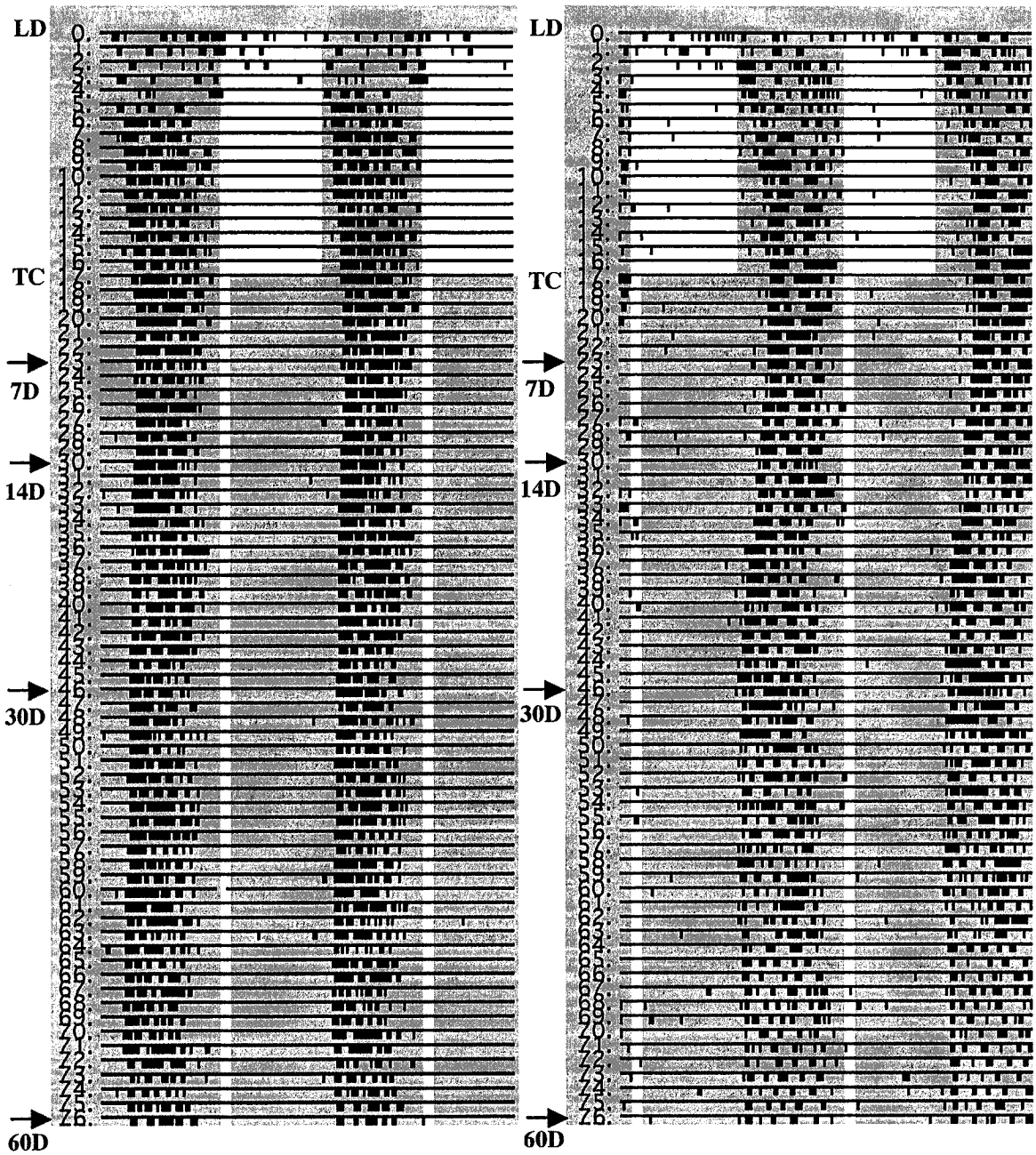

Figure 1. Representative double plotted actograms from 2 rats housed under a 24-h T-cycle for 60 days. LD= 12-h:12-h light:dark cycle, TC= T-cycle, and arrows indicate number of days on a T-cycle. Vertical white bars indicate lights on, grey background indicates lights off. Vertical marks indicate periods of activity of at least 10 wheel revolutions/10 min. Successive days are plotted from top to bottom.

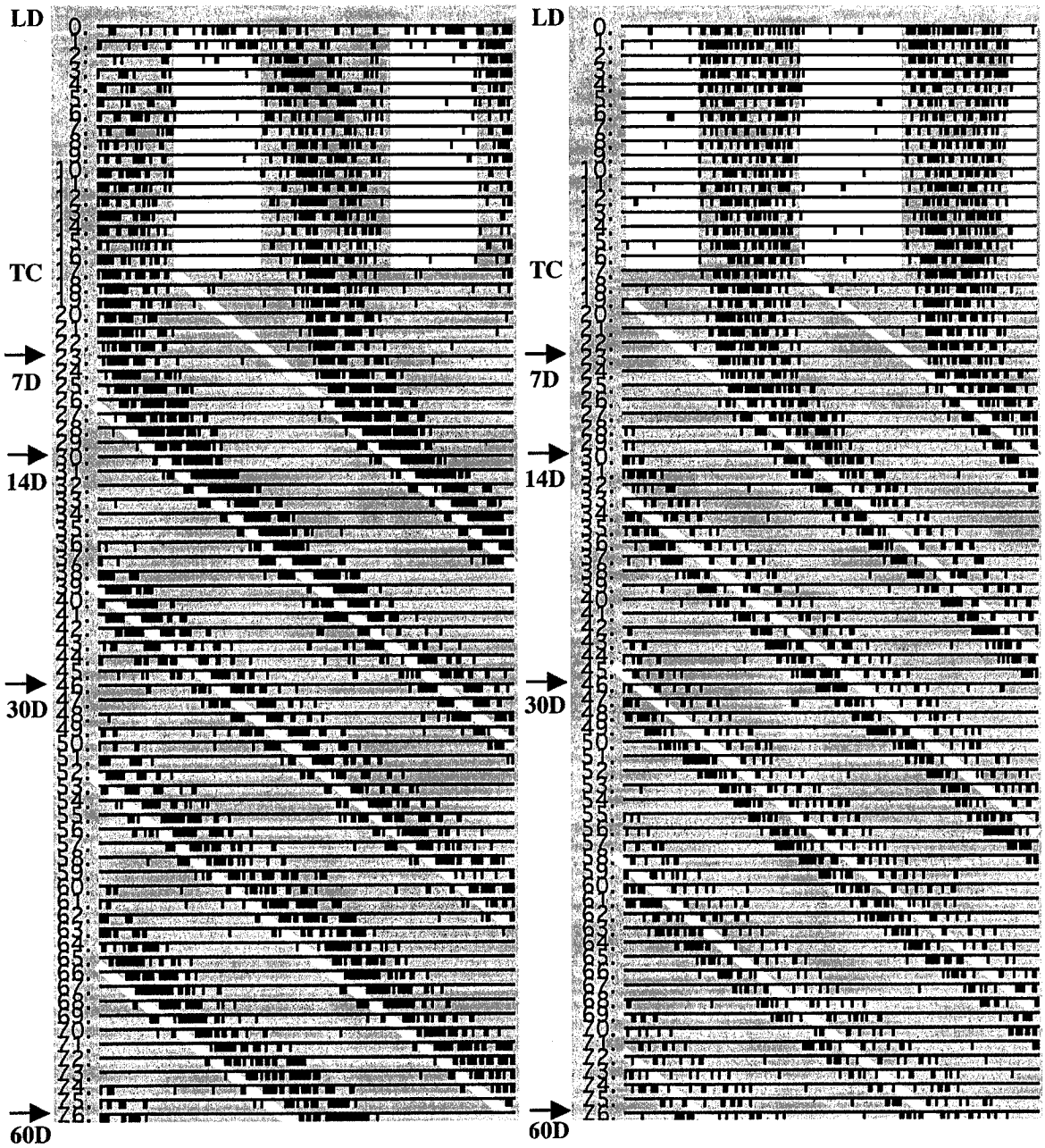

Figure 2. Representative double plotted actograms from 2 rats housed under a 26-h T-cycle for 60 days. LD= 12-h:12-h ligh/:dark cycle, TC= T-cycle, and arrows indicate number of days on a T-cycle. Vertical white bars indicate lights on, grey background indicates lights off. Vertical marks indicate periods of activity of at least 10 wheel revolutions/10 min. Successive days are plotted from top to bottom.

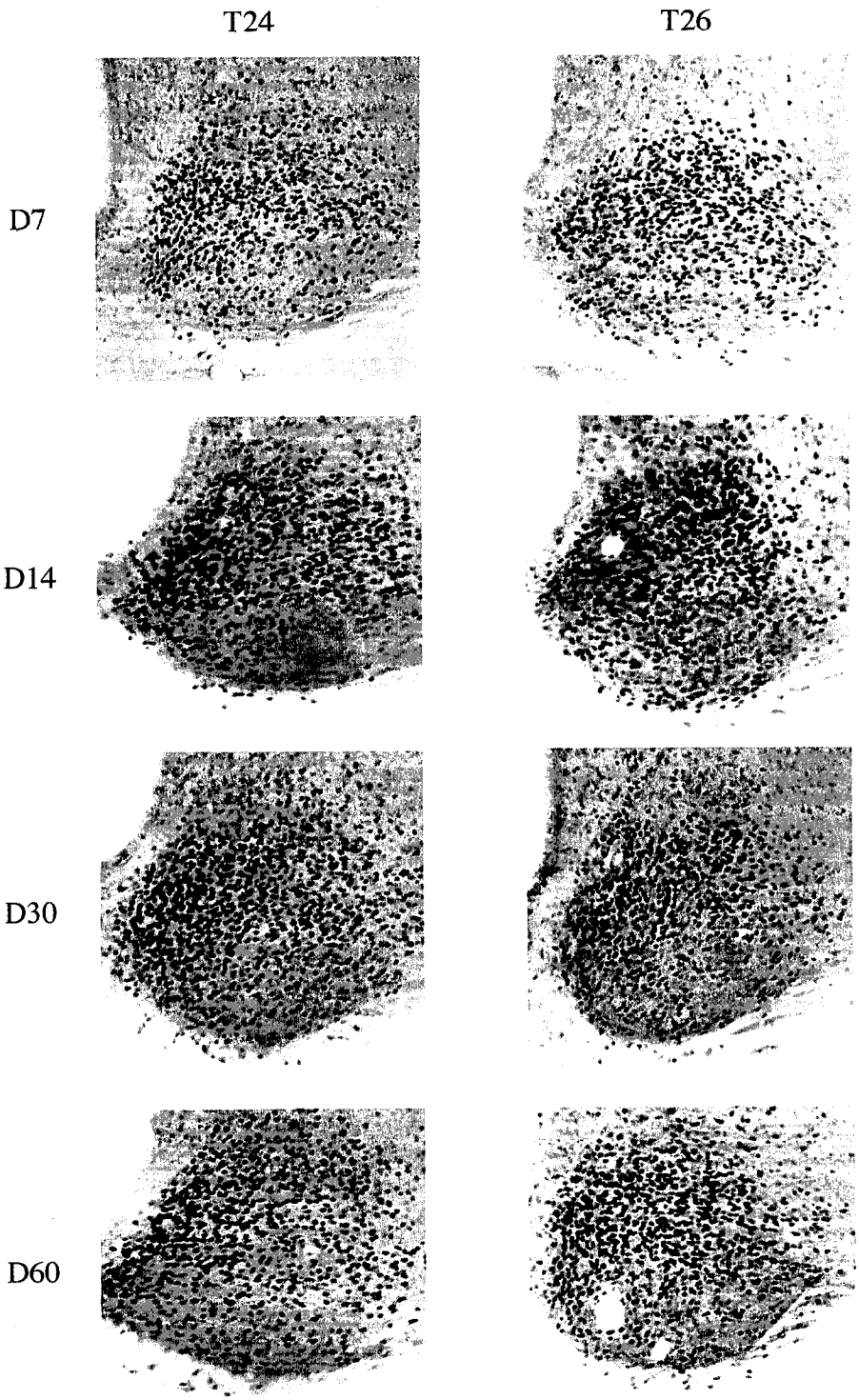

Figure 3. Representative photomicrographs of PER2 immunostaining in the SCN of rats kept on either a T24 (left column) or T26 (right column) cycle for 7, 14, 30, or 60 days, and sacrificed at activity onset.

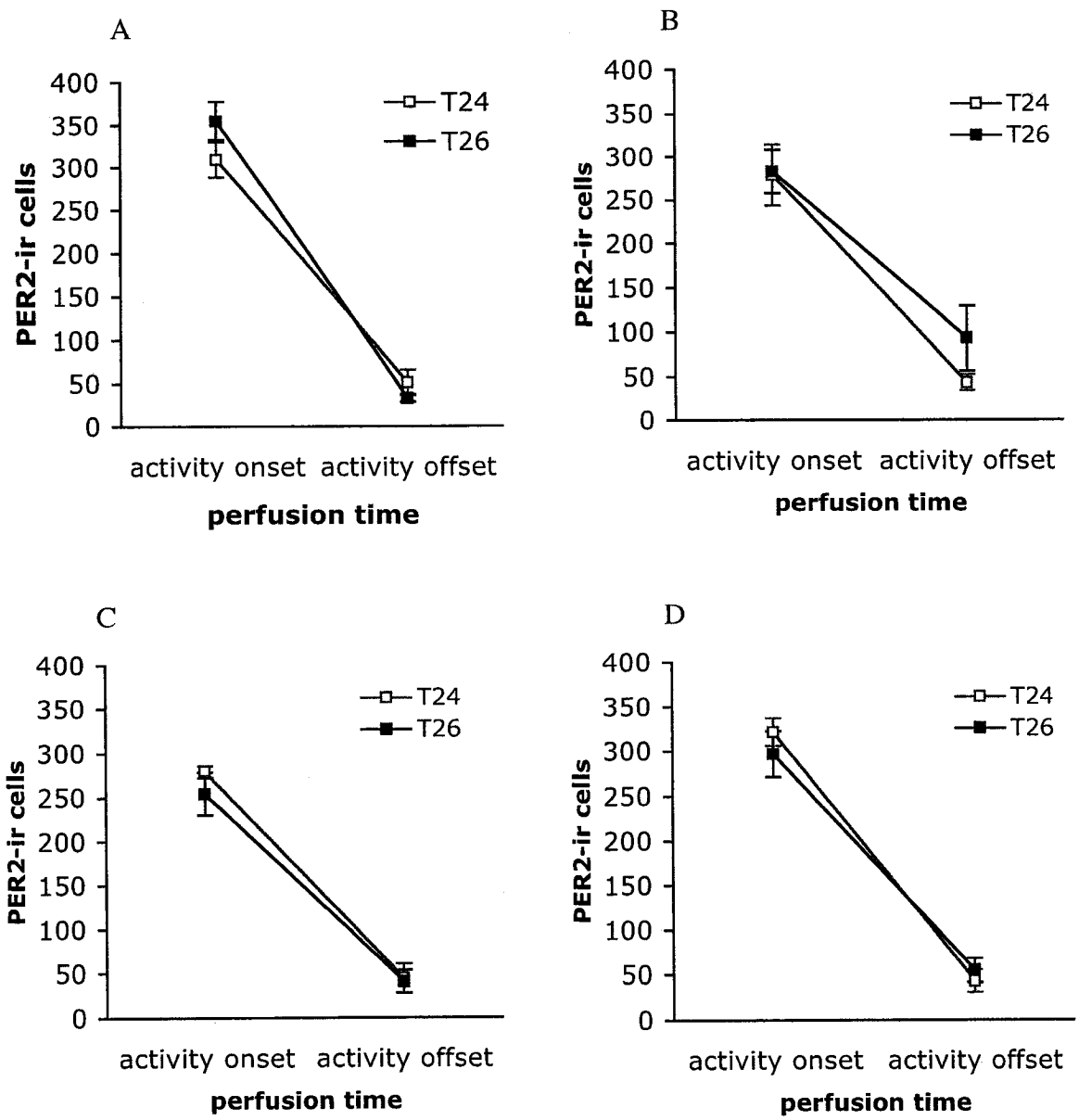

Figure 4. Mean (±SEM) number of PER2 immunoreactive cells in the SCN of rats killed at activity onset or offset, 7 days (A), 14 days (B), 30 days (C) or 60 days (D) after housing under a T24 (open squares) or T26 (filled squares) LD cycle (n=4/group).

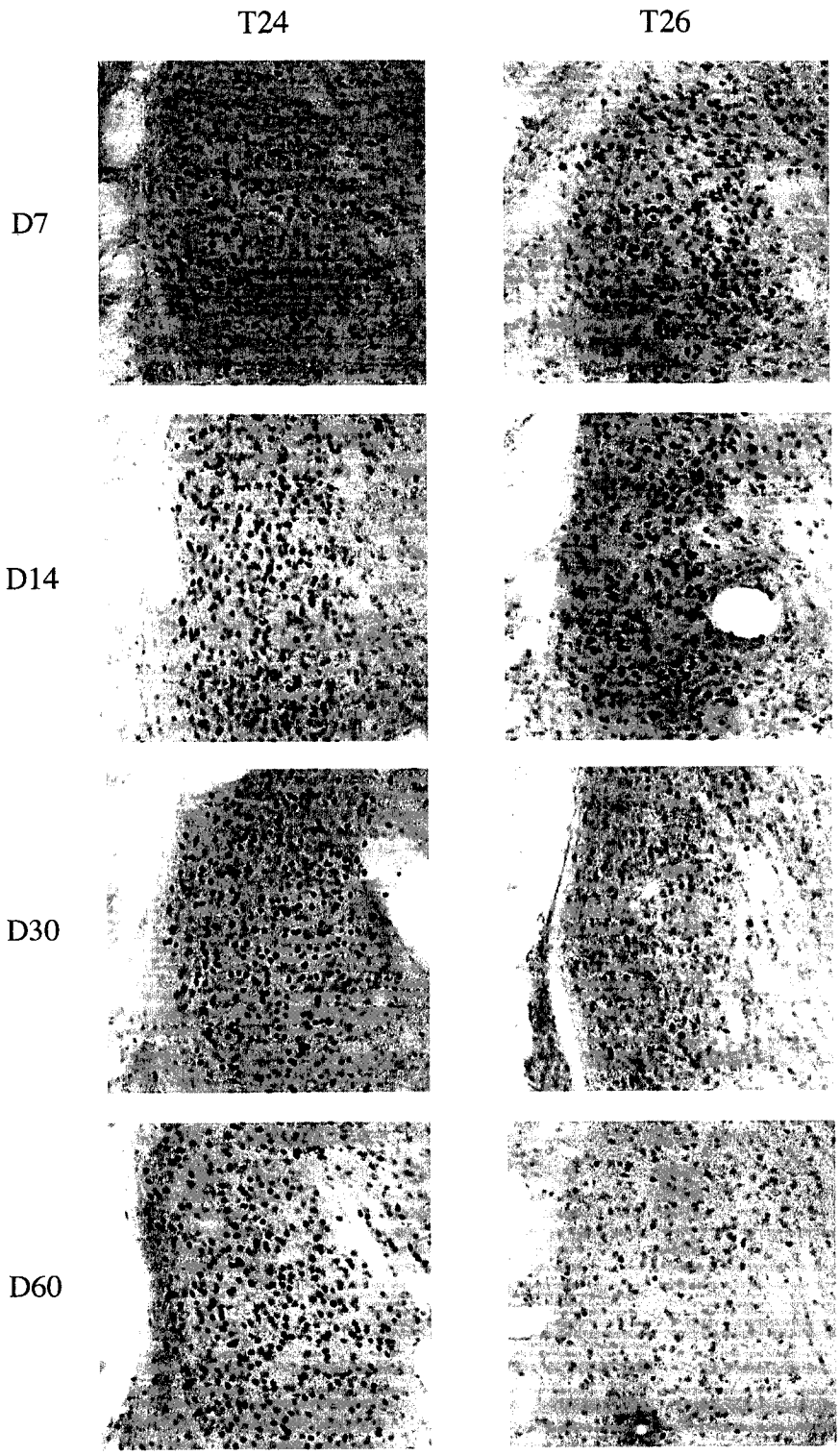

Figure 5. Representative photomicrographs of PER2 immunostaining in the BNSTov of rats kept on either a T24 (left column) or T26 (right column) cycle for 7, 14, 30, or 60 days, and sacrificed at activity onset.

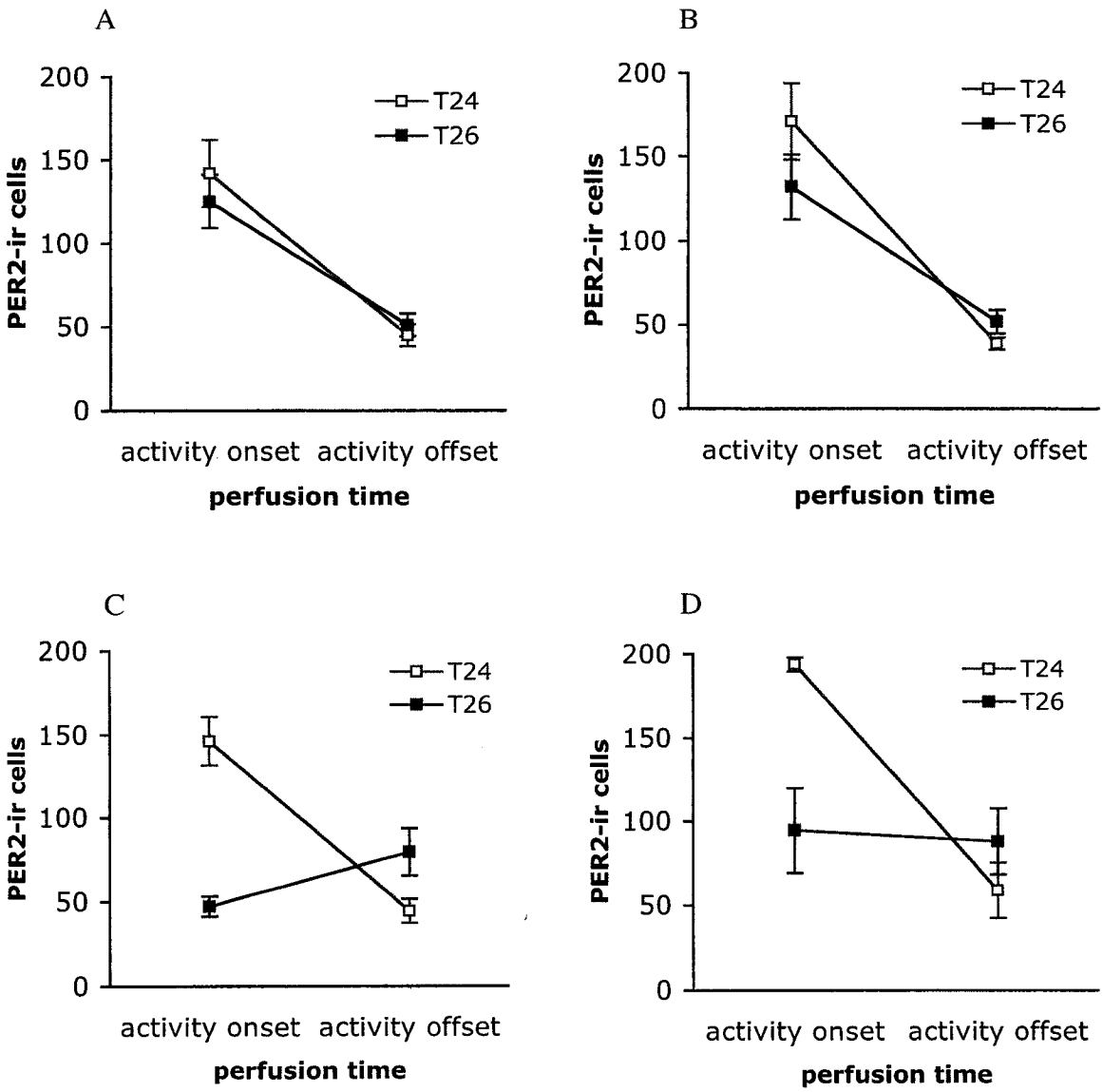

Figure 6. Mean (±SEM) number of PER2 immunoreactive cells in the BNSTov of rats killed at activity onset or offset, 7 days (A), 14 days (B), 30 days (C) or 60 days (D) after housing under a T24 (open squares) or T26 (filled squares) LD cycle (n=4/group).

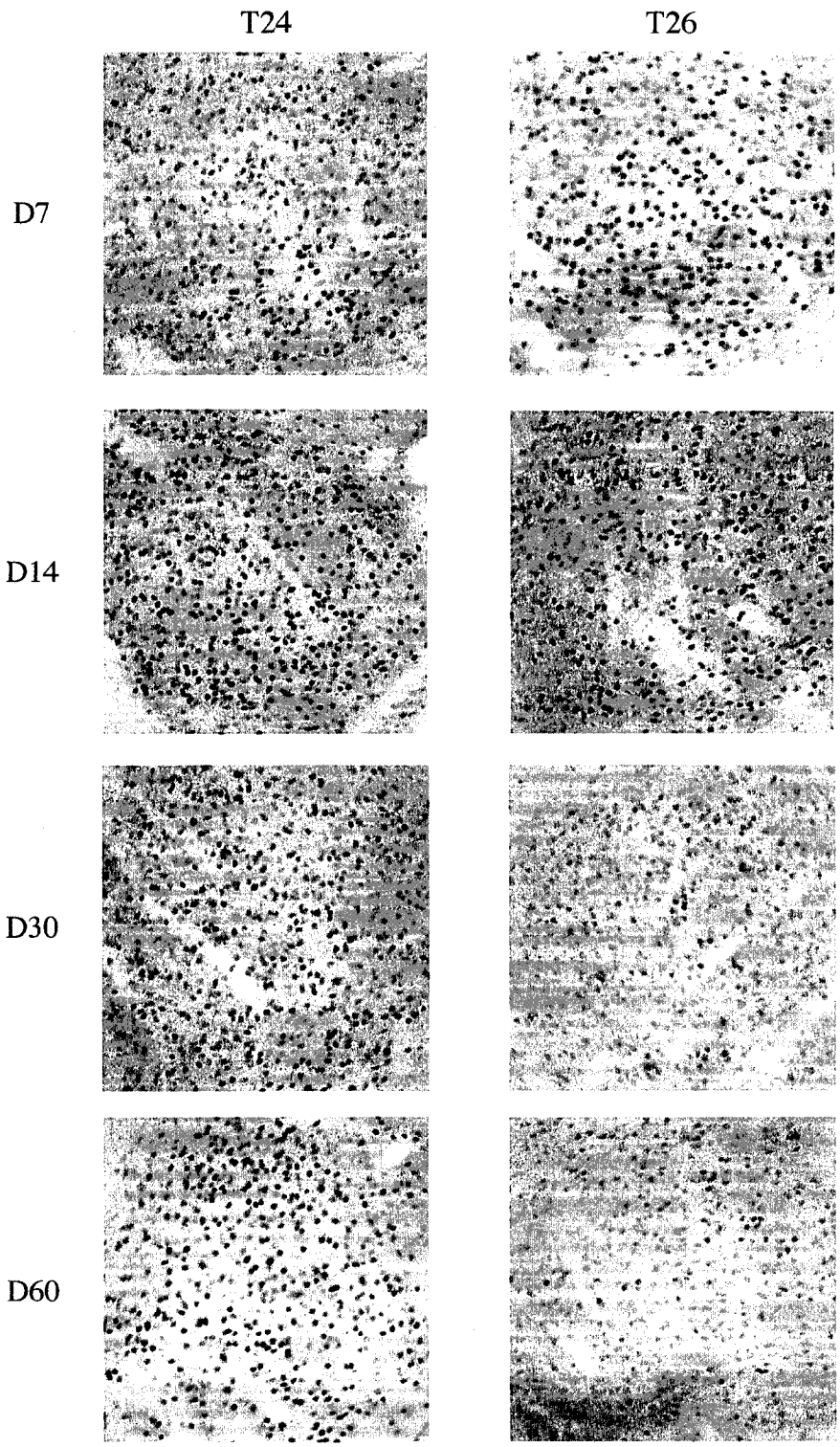

Figure 7. Representative photomicrographs of PER2 immunostaining in the CEA of rats kept on either a T24 (left column) or T26 (right column) cycle for 7, 14, 30, or 60 days, and sacrificed at activity onset.

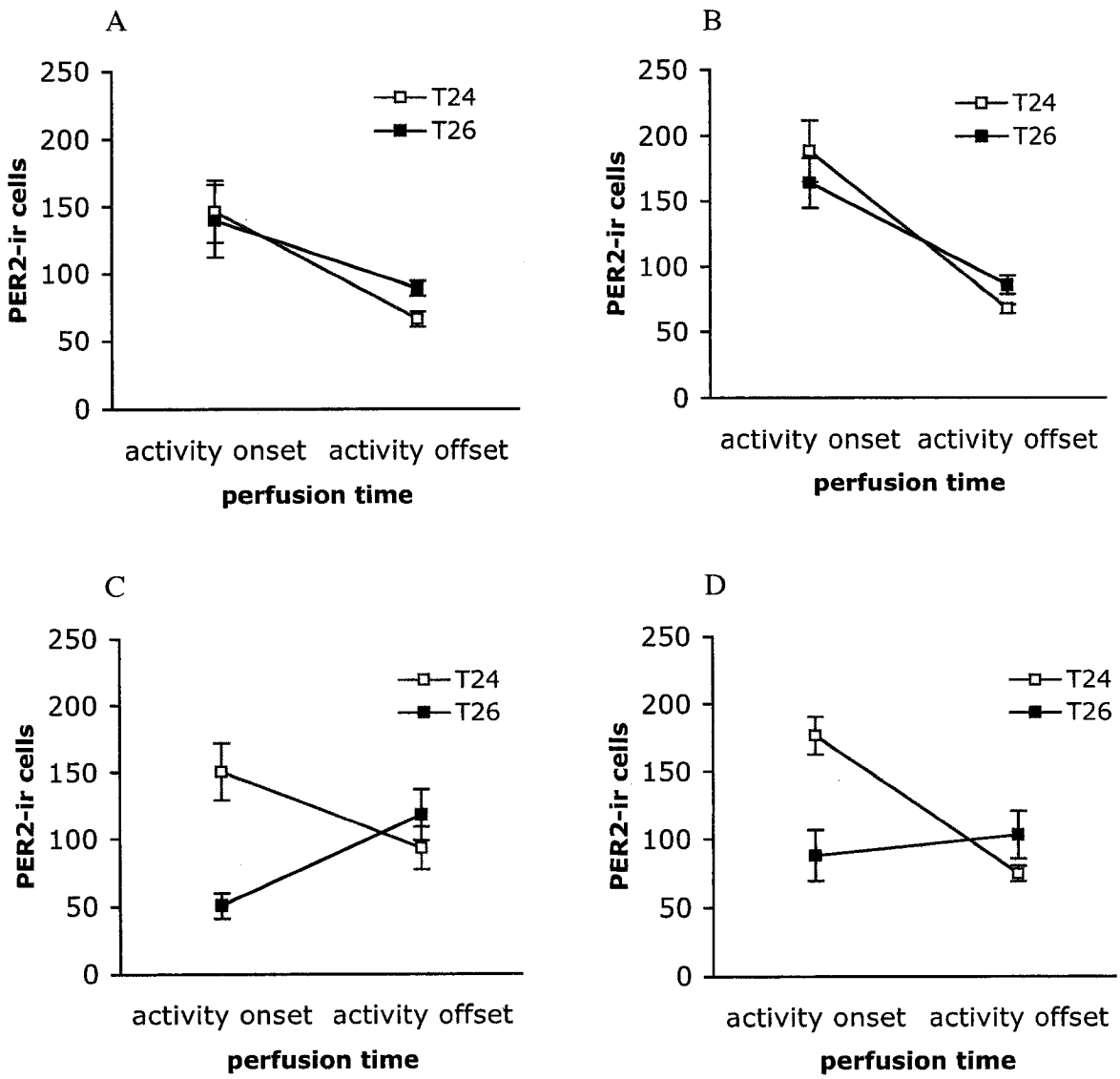

Figure 8. Mean (±SEM) number of PER2 immunoreactive cells in the CEA of rats killed at activity onset or offset, 7 days (A), 14 days (B), 30 days (C) or 60 days (D) after housing under a T24 (open squares) or T26 (filled squares) LD cycle (n=4/group).

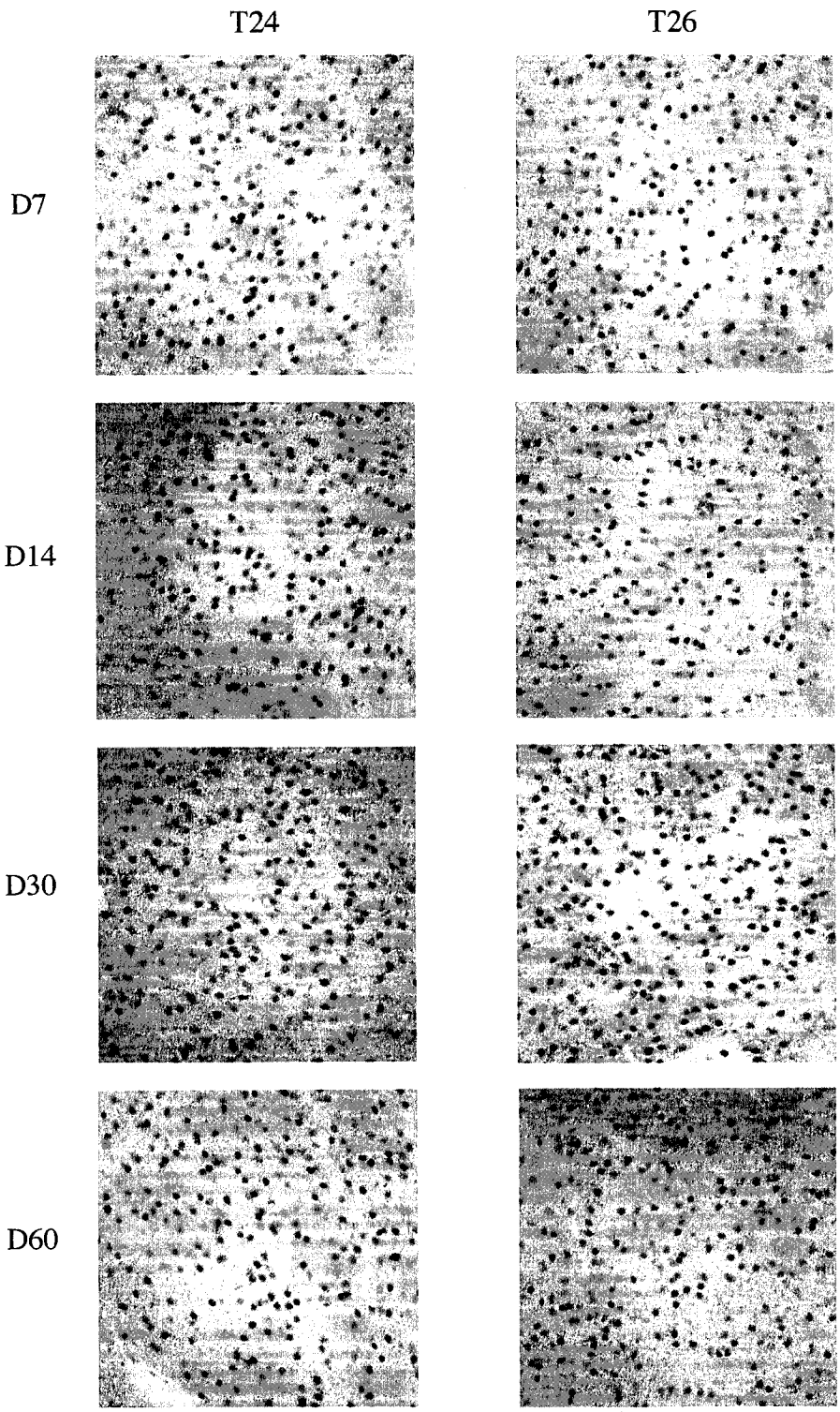

Figure 9. Representative photomicrographs of PER2 immunostaining in the BLA of rats kept on either a T24 (left column) or T26 (right column) cycle for 7, 14, 30, or 60 days, and sacrificed at activity offset.

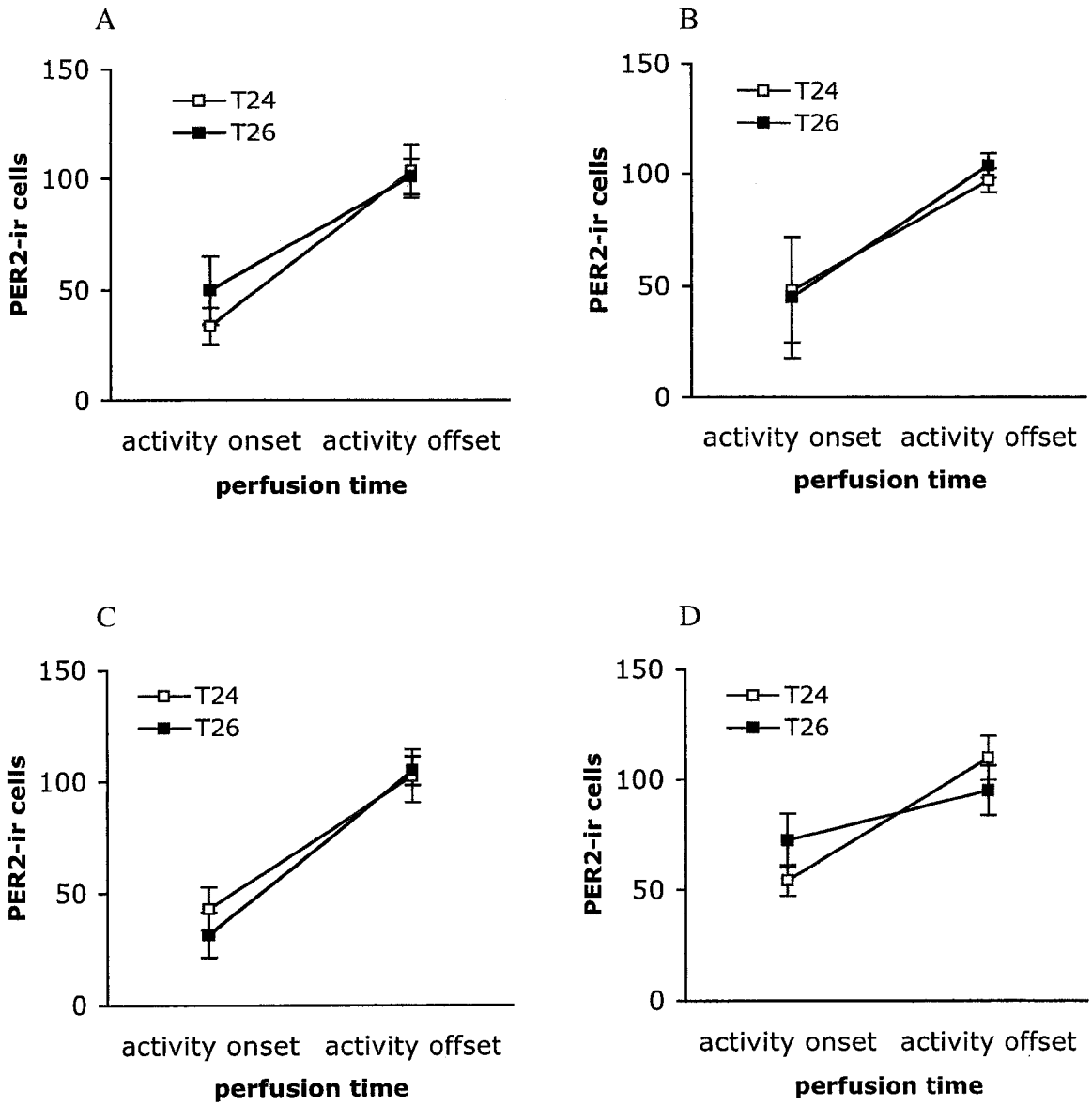

Figure 10. Mean (±SEM) number of PER2 immunoreactive cells in the BLA of rats killed at activity onset or offset, 7 days (A), 14 days (B), 30 days (C) or 60 days (D) after housing under a T24 (open squares) or T26 (filled squares) LD cycle (n=4/group).

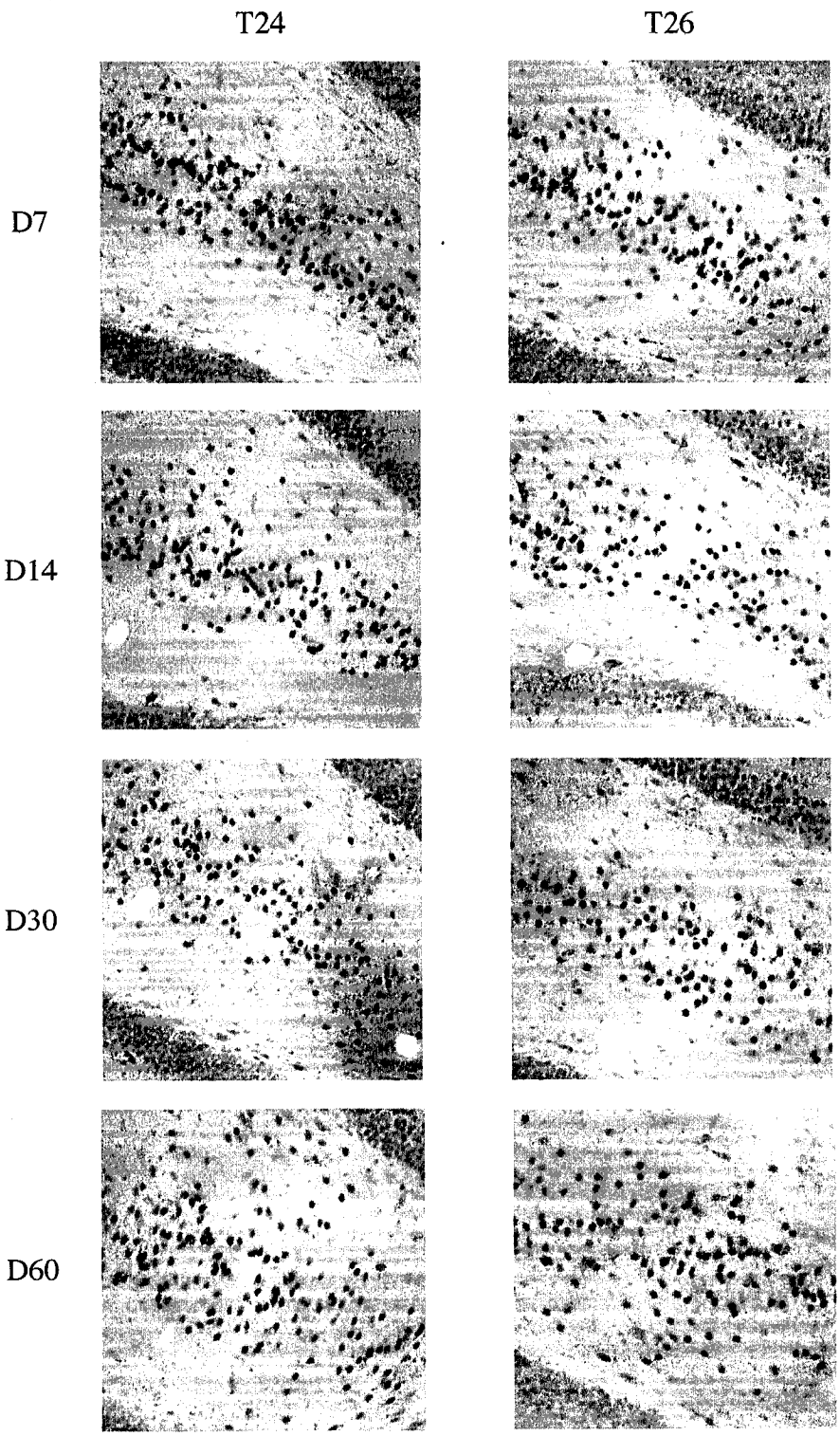

Figure 11. Representative photomicrographs of PER2 immunostaining in the DG of rats kept on either a T24 (left column) or T26 (right column) cycle for 7, 14, 30, or 60 days, and sacrificed at activity offset.

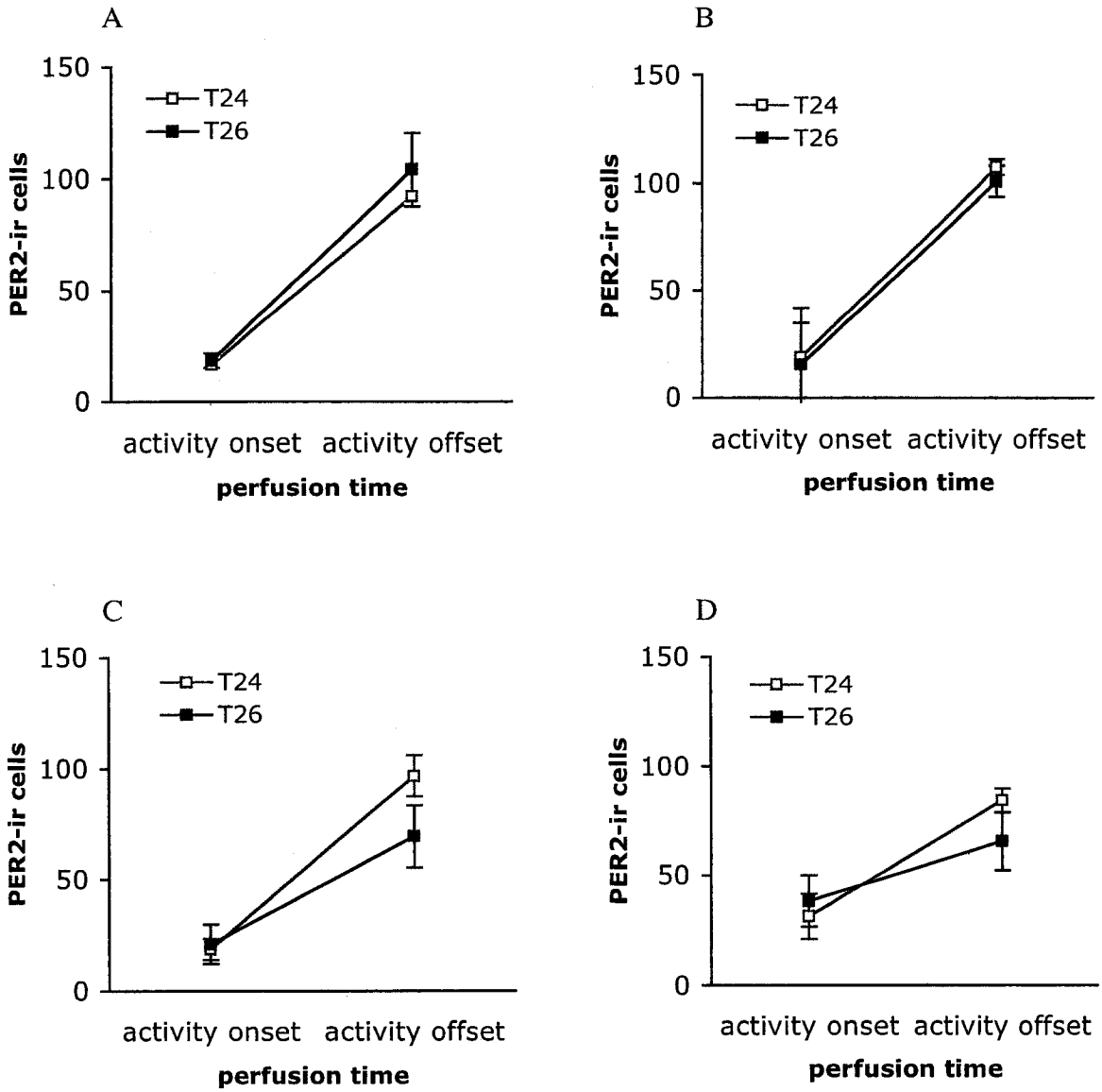

Figure 12. Mean (±SEM) number of PER2 immunoreactive cells in the DG of rats killed at activity onset or offset, 7 days (A), 14 days (B), 30 days (C) or 60 days (D) after housing under a T24 (open squares) or T26 (filled squares) LD cycle (n=4/group).

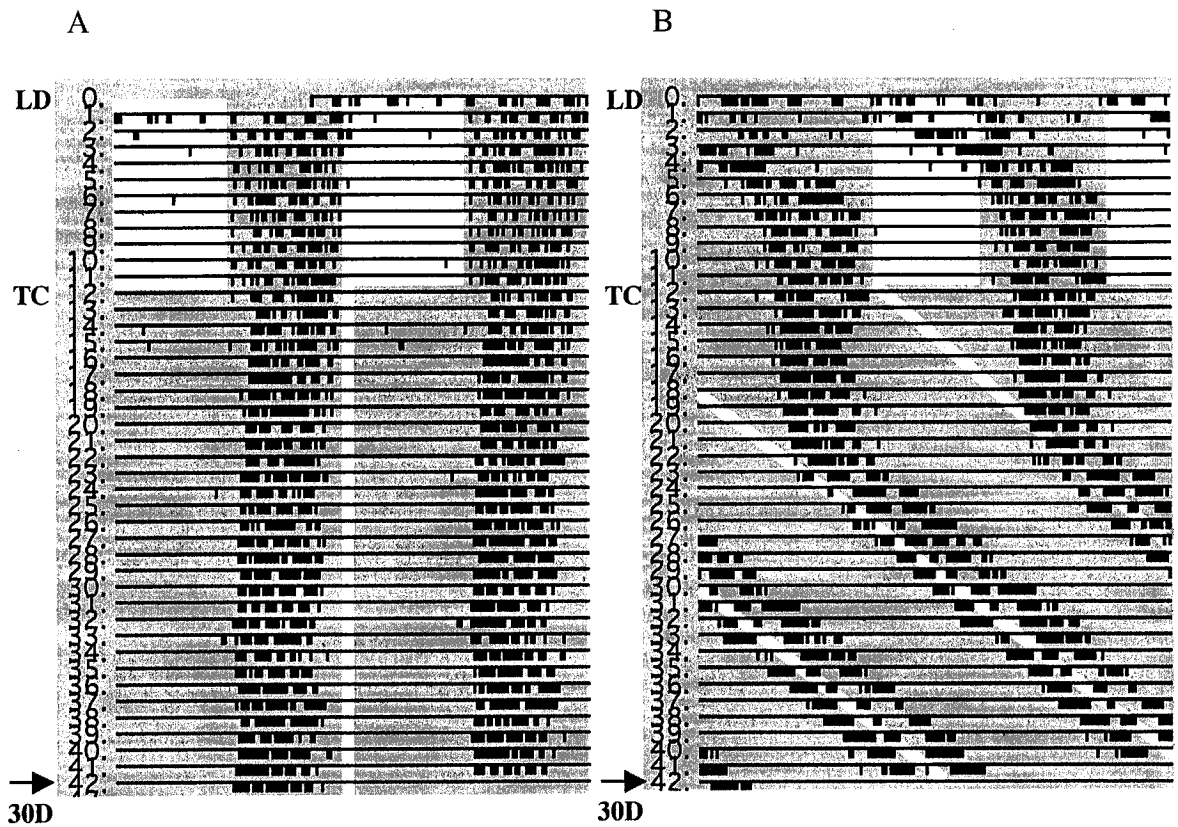

Figure 13. Representative double plotted actograms of rats housed under a 24-h T-cycle (A) or a 26-h T-cycle (B) for 30 days. LD= 12-h:12-h light:dark cycle, TC= T-cycle, and arrow indicates number of days on a T-cycle. Vertical white bars indicate lights on, grey background indicates lights off. Vertical marks indicate periods of activity of at least 10 wheel revolutions/10 min. Successive days are plotted from top to bottom.

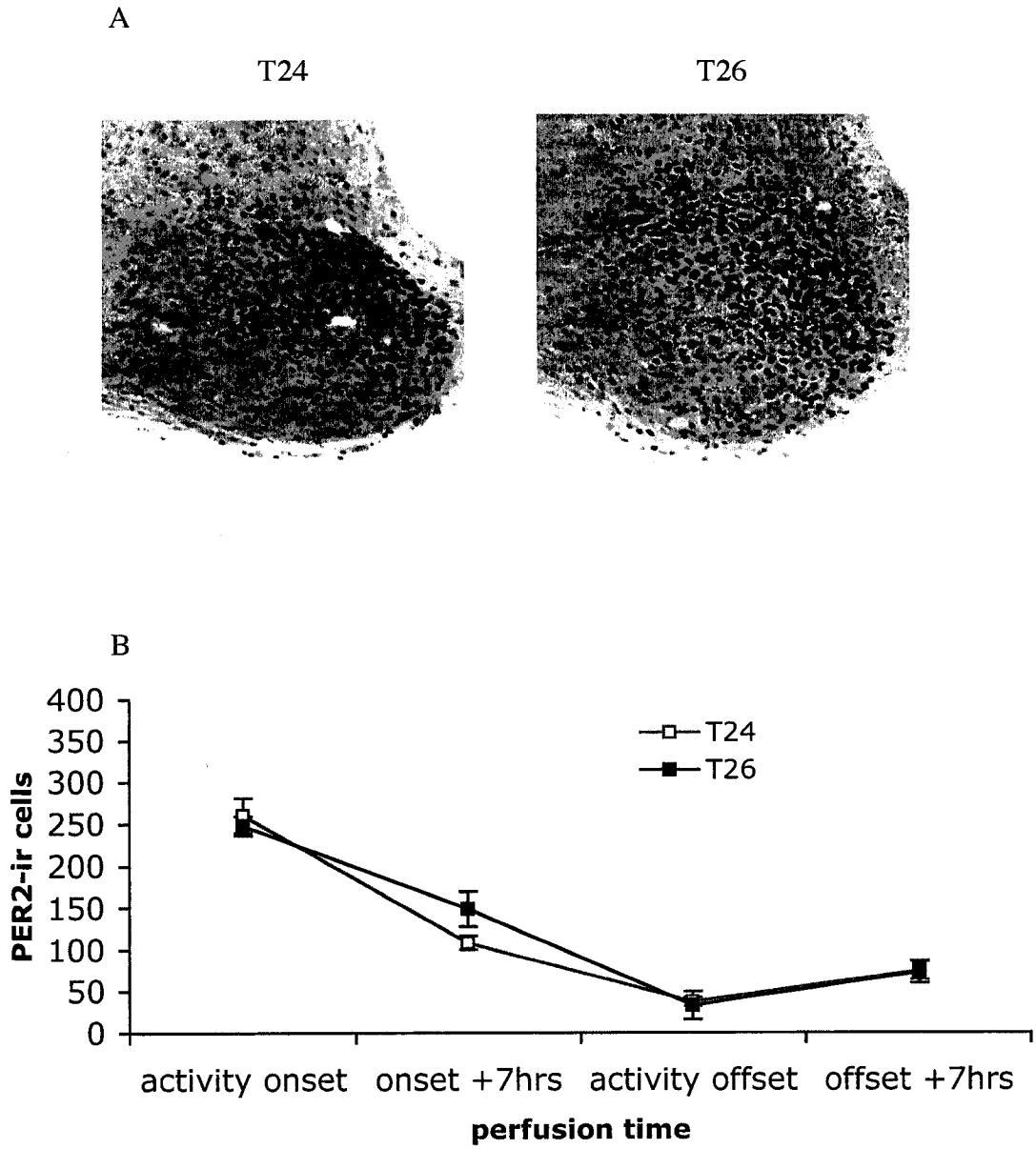

Figure 14. A) Representative photomicrographs of PER2 immunostaining in the SCN of rats kept on either a T24 (left) or T26 (right) cycle for 30 days and sacrificed at activity onset. B) Mean (±SEM) number of PER2 immunoreactive cells in the SCN of rats killed at activity onset, onset +7hrs, offset, or offset +7hrs, 30 days after housing under a T24 (open squares) or T26 (filled squares) LD cycle (n=3-5/group).

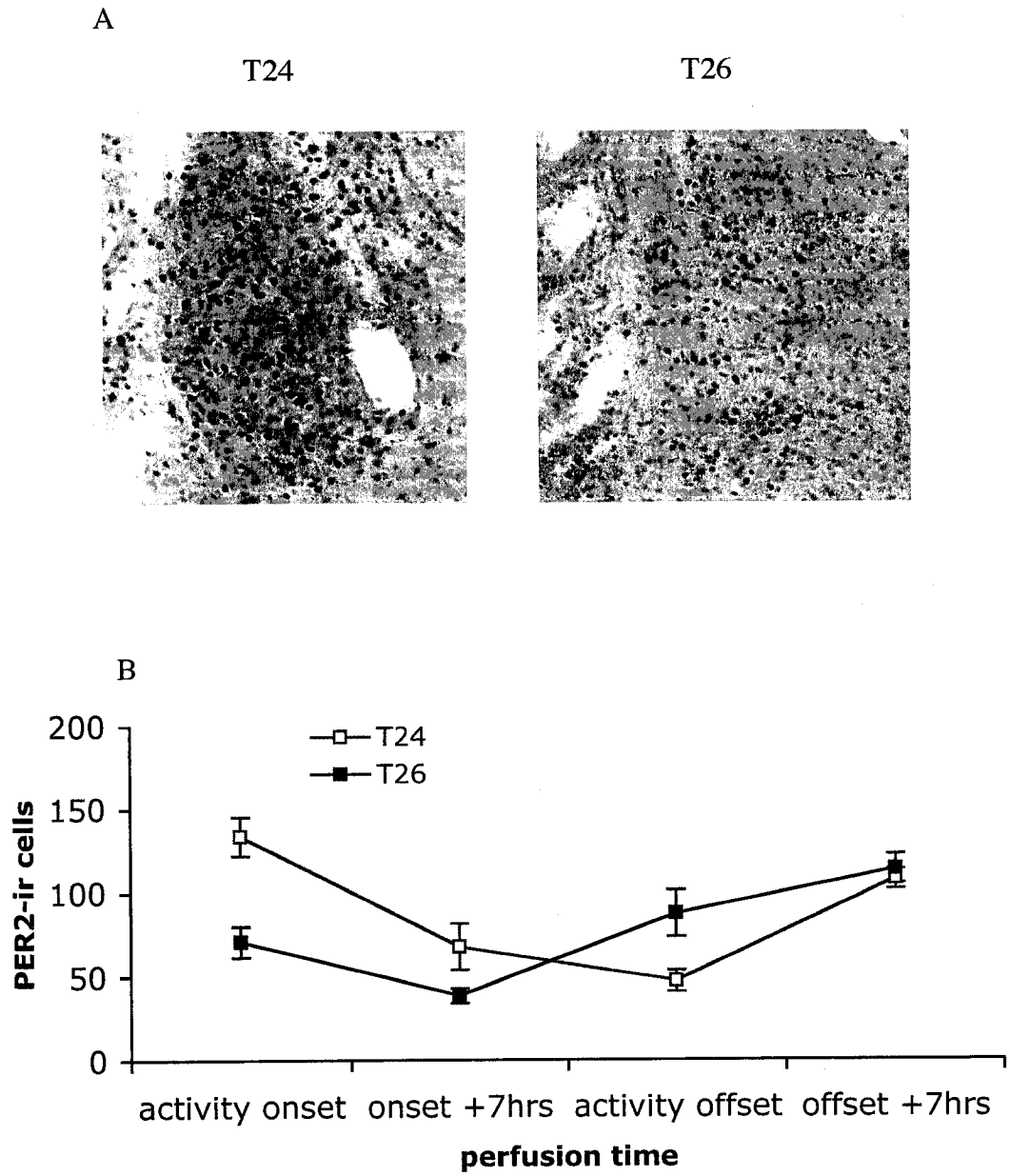

Figure 15. A) Representative photomicrographs of PER2 immunostaining in the BNSTov of rats kept on either a T24 (left) or T26 (right) cycle for 30 days and sacrificed at activity onset. B) Mean (±SEM) number of PER2 immunoreactive cells in the BNSTov of rats killed at activity onset, onset +7hrs, offset, or offset +7hrs, 30 days after housing under a T24 (open squares) or T26 (filled squares) LD cycle (n=3-5/group).

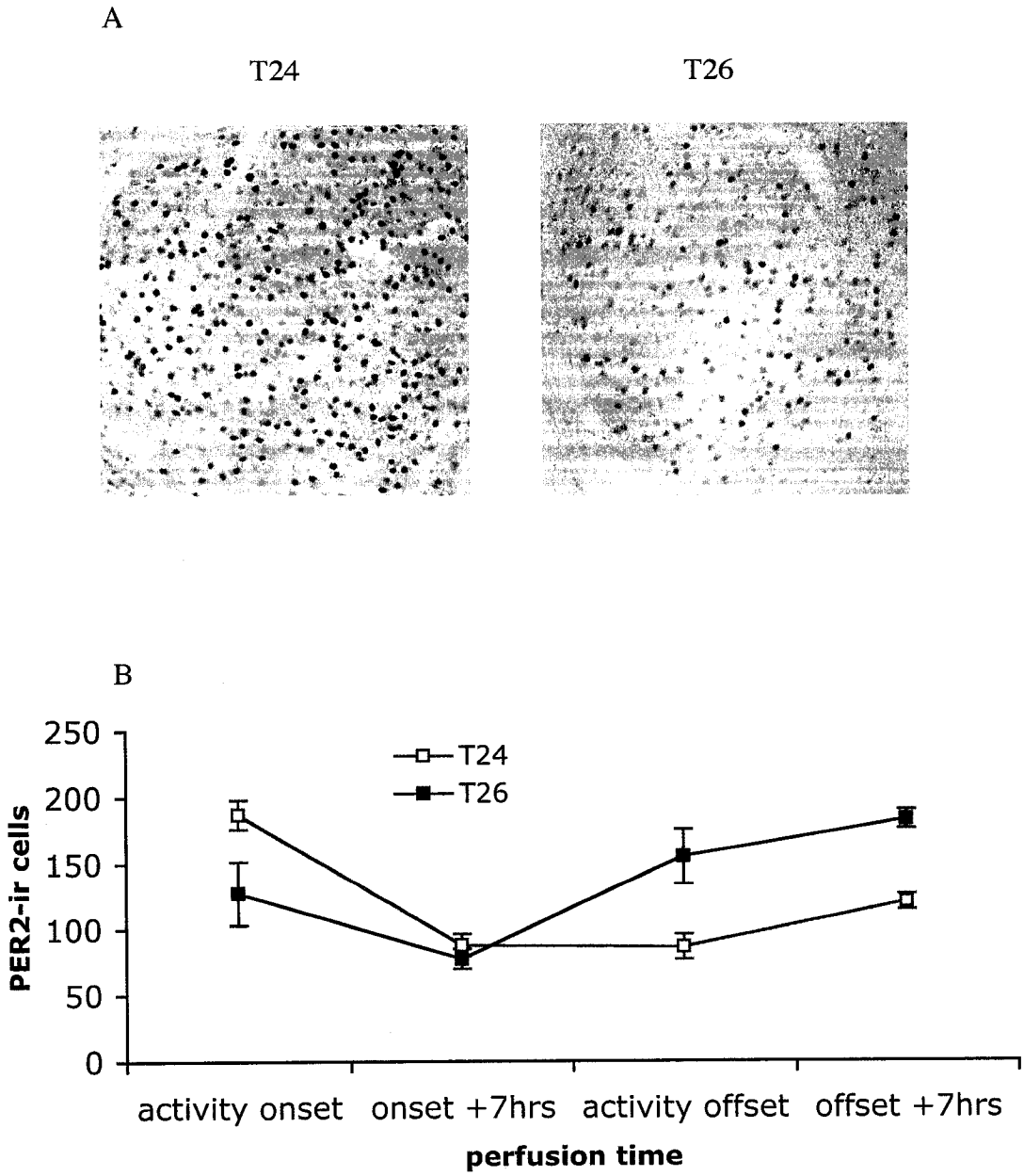

Figure 16. A) Representative photomicrographs of PER2 immunostaining in the CEA of rats kept on either a T24 (left) or T26 (right) cycle for 30 days and sacrificed at activity onset. B) Mean (±SEM) number of PER2 immunoreactive cells in the CEA of rats killed at activity onset, onset +7hrs, offset, or offset +7hrs, 30 days after housing under a T24 (open squares) or T26 (filled squares) LD cycle (n=3-5/group).

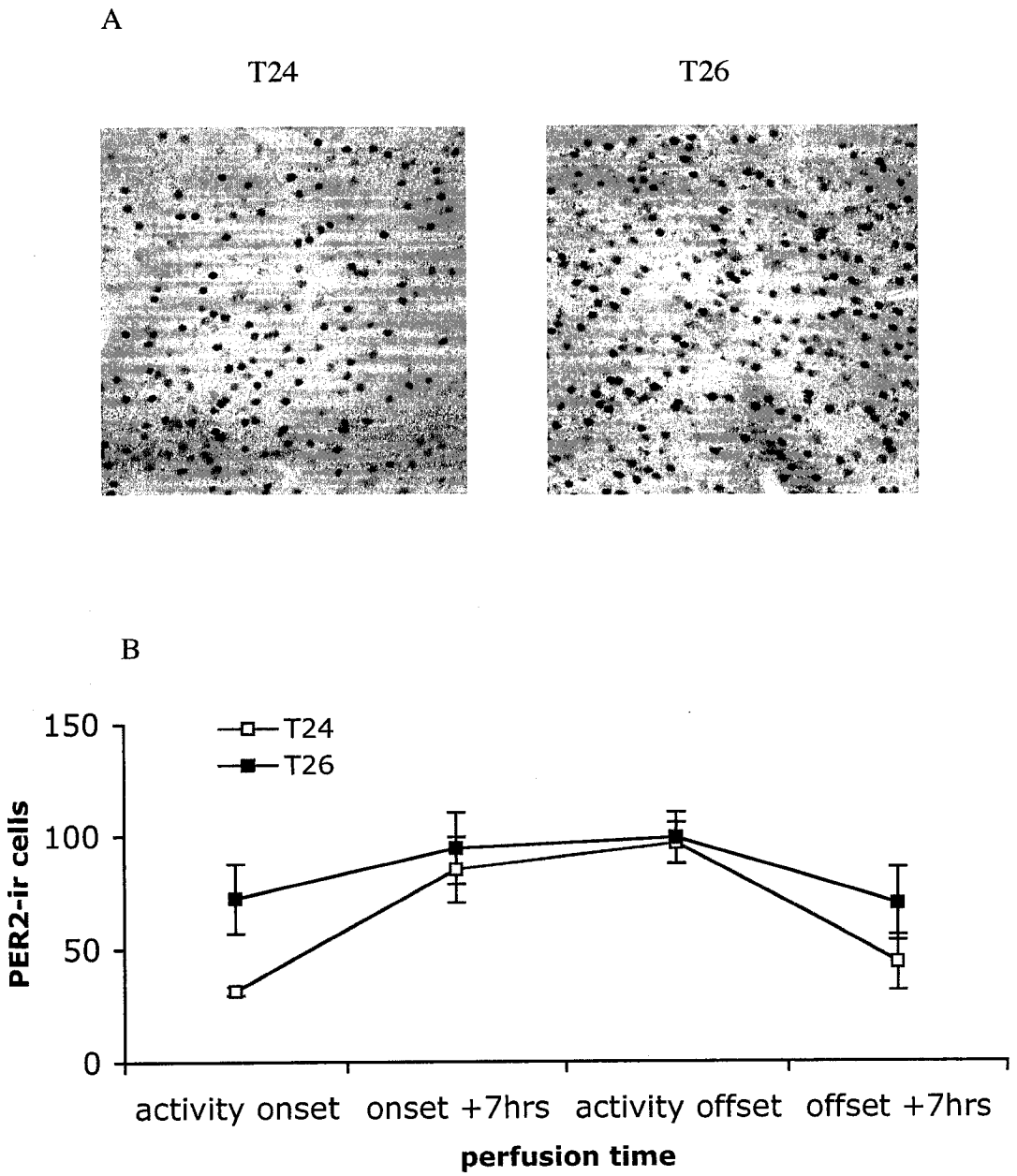

Figure 17. A) Representative photomicrographs of PER2 immunostaining in the BLA of rats kept on either a T24 (left) or T26 (right) cycle for 30 days and sacrificed at activity offset. B) Mean (±SEM) number of PER2 immunoreactive cells in the BLA of rats killed at activity onset, onset +7hrs, offset, or offset +7hrs, 30 days after housing under a T24 (open squares) or T26 (filled squares) LD cycle (n=3-5/group).

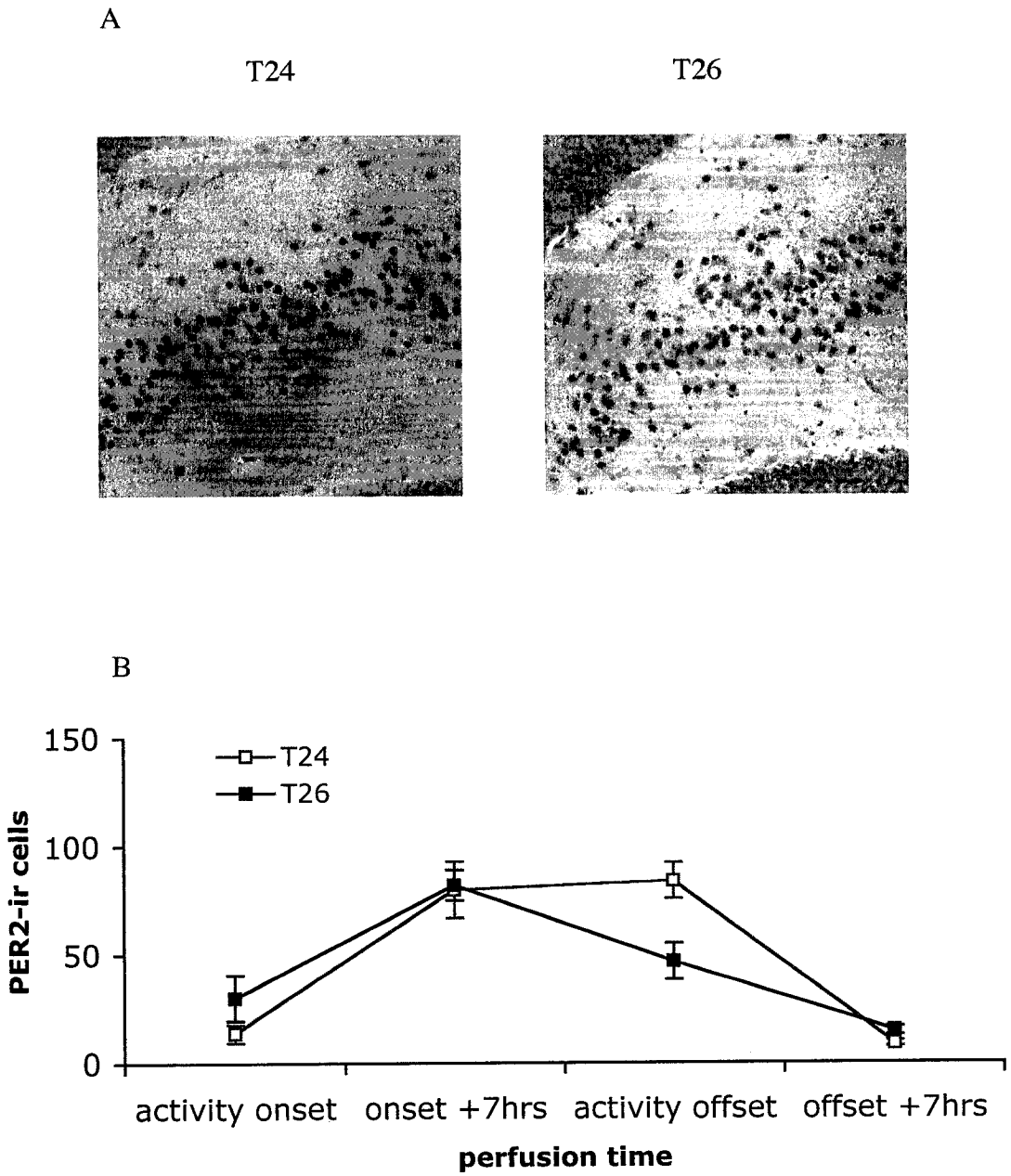

Figure 18. A) Representative photomicrographs of PER2 immunostaining in the DG of rats kept on either a T24 (left) or T26 (right) cycle for 30 days and sacrificed at activity offset. B) Mean (±SEM) number of PER2 immunoreactive cells in the DG of rats killed at activity onset, onset +7hrs, offset, or offset +7hrs, 30 days after housing under a T24 (open squares) or T26 (filled squares) LD cycle (n=3-5/group).

REFERENCES

Abe, M., Herzog, E. D., Yamazaki, S., Straume, M., Tei, H., Sakaki, Y., et al. (2002). Circadian rhythms in isolated brain regions. *J Neurosci, 22*(1), 350-356.

Amir, S., Harbour, V. L., & Robinson, B. (2006). Pinealectomy does not affect diurnal PER2 expression in the rat limbic forebrain. *Neurosci Lett.*

Amir, S., Lamont, E. W., Robinson, B., & Stewart, J. (2004). A circadian rhythm in the expression of PERIOD2 protein reveals a novel SCN-controlled oscillator in the oval nucleus of the bed nucleus of the stria terminalis. *J Neurosci, 24*(4), 781-790.

Bae, K., Jin, X., Maywood, E. S., Hastings, M. H., Reppert, S. M., & Weaver, D. R. (2001). Differential functions of mPer1, mPer2, and mPer3 in the SCN circadian clock. *Neuron, 30*(2), 525-536.

Beaule, C., Houle, L. M., & Amir, S. (2003). Expression profiles of PER2 immunoreactivity within the shell and core regions of the rat suprachiasmatic nucleus: lack of effect of photic entrainment and disruption by constant light. *J Mol Neurosci, 21*(2), 133-147.

Boulos, Z., & Terman, M. (1980). Food availability and daily biological rhythms. *Neurosci Biobehav Rev, 4*(2), 119-131.

Bunney, W. E., & Bunney, B. G. (2000). Molecular clock genes in man and lower animals: possible implications for circadian abnormalities in depression. *Neuropsychopharmacology, 22*(4), 335-345.

Cassone, V. M., Warren, W. S., Brooks, D. S., & Lu, J. (1993). Melatonin, the pineal gland, and circadian rhythms. *J Biol Rhythms, 8 Suppl*, S73-81.

Challet, E., Caldelas, I., Graff, C., & Pevet, P. (2003). Synchronization of the molecular clockwork by light- and food-related cues in mammals. *Biol Chem, 384*(5), 711-719.

Davis, M. (1998). Are different parts of the extended amygdala involved in fear versus anxiety? *Biol Psychiatry, 44*(12), 1239-1247.

Day, H. E., Badiani, A., Uslaner, J. M., Oates, M. M., Vittoz, N. M., Robinson, T. E., et al. (2001). Environmental novelty differentially affects c-fos mRNA expression induced by amphetamine or cocaine in subregions of the bed nucleus of the stria terminalis and amygdala. *J Neurosci, 21*(2), 732-740.

Day, H. E., Curran, E. J., Watson, S. J., Jr., & Akil, H. (1999). Distinct neurochemical populations in the rat central nucleus of the amygdala and bed nucleus of the stria terminalis: evidence for their selective activation by interleukin-1beta. *J Comp Neurol, 413*(1), 113-128.

Dong, H. W., Petrovich, G. D., & Swanson, L. W. (2001). Topography of projections from amygdala to bed nuclei of the stria terminalis. *Brain Res Brain Res Rev, 38*(1-2), 192-246.

Dong, H. W., Petrovich, G. D., Watts, A. G., & Swanson, L. W. (2001). Basic organization of projections from the oval and fusiform nuclei of the bed nuclei of the stria terminalis in adult rat brain. *J Comp Neurol, 436*(4), 430-455.

Erb, S., Salmaso, N., Rodaros, D., & Stewart, J. (2001). A role for the CRF-containing pathway from central nucleus of the amygdala to bed nucleus of the stria terminalis in the stress-induced reinstatement of cocaine seeking in rats. *Psychopharmacology (Berl), 158*(4), 360-365.

Erb, S., Shaham, Y., & Stewart, J. (2001). Stress-induced relapse to drug seeking in the rat: Role of the bed nucleus of the stria terminalis and amygdala. *Stress, 4*, 289-303.

Hogenesch, J. B., Panda, S., Kay, S., & Takahashi, J. S. (2003). Circadian transcriptional output in the SCN and liver of the mouse. *Novartis Found Symp, 253*, 171-180; discussion 152-175, 102-179, 180-173 passim.

Jilg, A., Moek, J., Weaver, D. R., Korf, H. W., Stehle, J. H., & von Gall, C. (2005). Rhythms in clock proteins in the mouse pars tuberalis depend on MT1 melatonin receptor signalling. *Eur J Neurosci, 22*(11), 2845-2854.

Ko, C. H., & Takahashi, J. S. (2006). Molecular components of the mammalian circadian clock. *Hum Mol Genet, 15 Spec No 2*, R271-277.

Lamont, E. W., Diaz, L. R., Barry-Shaw, J., Stewart, J., & Amir, S. (2005). Daily restricted feeding rescues a rhythm of period2 expression in the arrhythmic suprachiasmatic nucleus. *Neuroscience, 132*(2), 245-248.

Lamont, E. W., Robinson, B., Stewart, J., & Amir, S. (2005). The central and basolateral nuclei of the amygdala exhibit opposite diurnal rhythms of expression of the clock protein Period2. *Proc Natl Acad Sci U S A, 102*(11), 4180-4184.

Laudon, M., Nir, I., & Zisapel, N. (1988). Melatonin receptors in discrete brain areas of the male rat. Impact of aging on density and on circadian rhythmicity. *Neuroendocrinology, 48*(6), 577-583.

Lee, Y., & Davis, M. (1997). Role of the hippocampus, the bed nucleus of the stria terminalis, and the amygdala in the excitatory effect of corticotropin-releasing hormone on the acoustic startle reflex. *J Neurosci, 17*(16), 6434-6446.

Lehman, M. N., Silver, R., Gladstone, W. R., Kahn, R. M., Gibson, M., & Bittman, E. L. (1987). Circadian rhythmicity restored by neural transplant. Immunocytochemical characterization of the graft and its integration with the host brain. *J Neurosci, 7*(6), 1626-1638.

Lowrey, P. L., & Takahashi, J. S. (2000). Genetics of the mammalian circadian system: Photic entrainment, circadian pacemaker mechanisms, and posttranslational regulation. *Annu Rev Genet, 34*, 533-562.

Masubuchi, S., Kataoka, N., Sassone-Corsi, P., & Okamura, H. (2005). Mouse Period1 (mPER1) acts as a circadian adaptor to entrain the oscillator to environmental light/dark cycles by regulating mPER2 protein. *J Neurosci, 25*(19), 4719-4724.

Mistlberger, R. E. (1994). Circadian food-anticipatory activity: formal models and physiological mechanisms. *Neurosci Biobehav Rev, 18*(2), 171-195.

Moore, R. Y., & Lenn, N. J. (1972). A retinohypothalamic projection in the rat. *J Comp Neurol, 146*(1), 1-14.

Musshoff, U., Riewenherm, D., Berger, E., Fauteck, J. D., & Speckmann, E. J. (2002). Melatonin receptors in rat hippocampus: molecular and functional investigations. *Hippocampus, 12*(2), 165-173.

Okamura, H., Yamaguchi, S., & Yagita, K. (2002). Molecular machinery of the circadian clock in mammals. *Cell Tissue Res, 309*(1), 47-56.

Petrovich, G. D., Canteras, N. S., & Swanson, L. W. (2001). Combinatorial amygdalar inputs to hippocampal domains and hypothalamic behavior systems. *Brain Res Brain Res Rev, 38*(1-2), 247-289.

Petrovich, G. D., & Gallagher, M. (2003). Amygdala subsystems and control of feeding behavior by learned cues. *Ann N Y Acad Sci, 985*, 251-262.

Pittendrigh, C. S., & Daan, S. (1976). A funtional analysis of circadian pacemakers in nocturnal rodents. *J. Comp. Physiol., 106*, 291-331.

Ralph, M. R., Foster, R. G., Davis, F. C., & Menaker, M. (1990). Transplanted suprachiasmatic nucleus determines circadian period. *Science, 247*(4945), 975-978.

Renteria Diaz, L., & Arvanitogiannis, A. Entrainment to a long daily cycle blocks behavioral sensitiaztion to cocaine. *Program No. 452.4. 2005 Abstract Viewer/Itinerary Planner, Washington, DC: SfN, 2005. Online.*

Renteria Diaz, L., & Arvanitogiannis, A. Entrainment to a long daily cycle reduces the reward value of cocaine. *Program No. 590.15. 2006 Abstract Viewer/Itinerary Planner, Atlanta, GA: SfN, 2006. Online.*

Rusak, B., & Zucker, I. (1979). Neural regulation of circadian rhythms. *Physiol Rev, 59*(3), 449-526.

Segall, L. A., Perrin, J. S., Walker, C. D., Stewart, J., & Amir, S. (2006). Glucocorticoid rhythms control the rhythm of expression of the clock protein, Period2, in oval

nucleus of the bed nucleus of the stria terminalis and central nucleus of the amygdala in rats. *Neuroscience, 140*(3), 753-757.

Stephan, F. K. (1983). Circadian rhythms in the rat: constant darkness, entrainment to T cycles and to skeleton photoperiods. *Physiol Behav, 30*(3), 451-462.

Stephan, F. K. (2002). The "other" circadian system: food as a Zeitgeber. *J Biol Rhythms, 17*(4), 284-292.

Stephan, F. K., & Zucker, I. (1972). Circadian rhythms in drinking behavior and locomotor activity of rats are eliminated by hypothalamic lesions. *Proc Natl Acad Sci U S A, 69*(6), 1583-1586.

Swanson, L. W. (2003). The amygdala and its place in the cerebral hemisphere. *Ann N Y Acad Sci, 985*, 174-184.

Tu, B. P., & McKnight, S. L. (2006). Metabolic cycles as an underlying basis of biological oscillations. *Nat Rev Mol Cell Biol, 7*(9), 696-701.

Uz, T., Akhisaroglu, M., Ahmed, R., & Manev, H. (2003). The pineal gland is critical for circadian Period1 expression in the striatum and for circadian cocaine sensitization in mice. *Neuropsychopharmacology, 28*(12), 2117-2123.

von Gall, C., Garabette, M. L., Kell, C. A., Frenzel, S., Dehghani, F., Schumm-Draeger, P. M., et al. (2002). Rhythmic gene expression in pituitary depends on heterologous sensitization by the neurohormone melatonin. *Nat Neurosci, 5*(3), 234-238.

Waddington Lamont, E., Harbour, V. L., Barry-Shaw, J., Renteria Diaz, L., Robinson, B., Stewart, J., et al. (2007). Restricted access to food, but not sucrose, saccharine, or salt, synchronizes the expression of Period2 protein in the limbic forebrain. *Neuroscience, 144*(2), 402-411.

Welsh, D. K., Logothetis, D. E., Meister, M., & Reppert, S. M. (1995). Individual neurons dissociated from rat suprachiasmatic nucleus express independently phased circadian firing rhythms. *Neuron, 14*(4), 697-706.

Yamazaki, S., Numano, R., Abe, M., Hida, A., Takahashi, R., Ueda, M., et al. (2000). Resetting central and peripheral circadian oscillators in transgenic rats. *Science, 288*(5466), 682-685.

Yoo, S. H., Yamazaki, S., Lowrey, P. L., Shimomura, K., Ko, C. H., Buhr, E. D., et al. (2004). PERIOD2::LUCIFERASE real-time reporting of circadian dynamics reveals persistent circadian oscillations in mouse peripheral tissues. *Proc Natl Acad Sci U S A, 101*(15), 5339-5346.

Zheng, B., Larkin, D. W., Albrecht, U., Sun, Z. S., Sage, M., Eichele, G., et al. (1999). The mPer2 gene encodes a functional component of the mammalian circadian clock. *Nature, 400*(6740), 169-173.

APPENDIX A

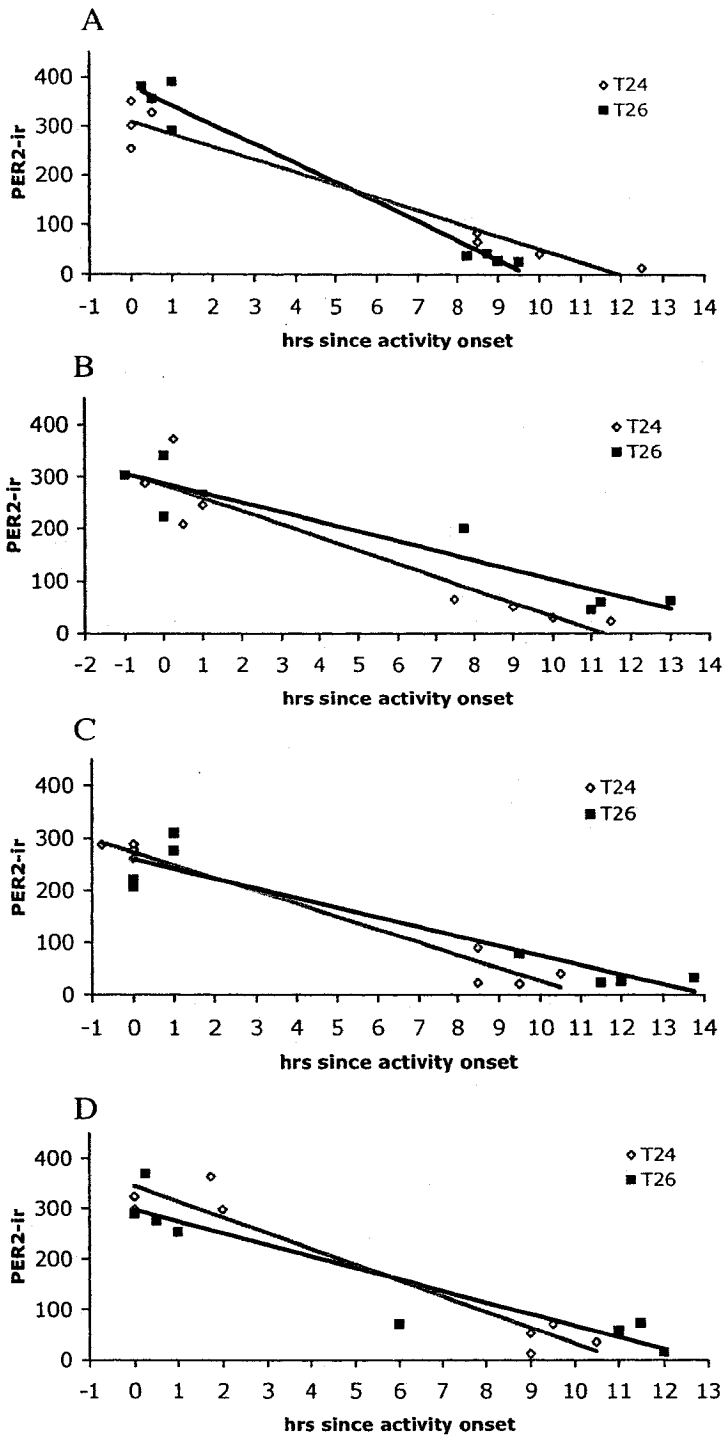

Figure A1. Scatterplot diagrams of PER2 immunoreactive cells in the SCN of individual rats under a T24 (open diamond) or T26 (filled square) for 7 (A), 14 (B), 30 (C), or 60 (D) days. Rats were killed at either activity onset (Hour 0) or activity offset, which varied according to the individual rat's activity pattern. Individual markers signify levels of PER2-ir versus time of perfusion for each rat.

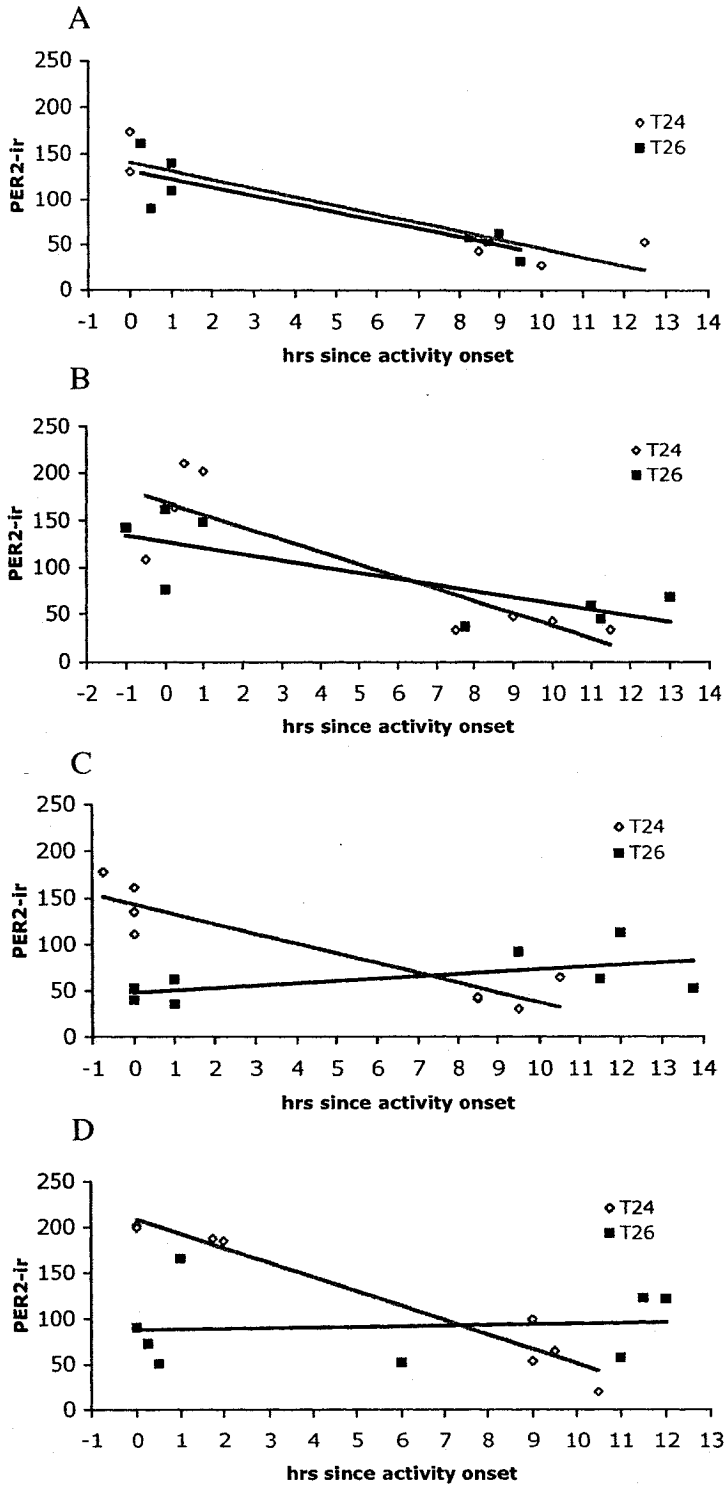

Figure A2. Scatterplot diagrams of PER2 immunoreactive cells in the BNSTov of individual rats under a T24 (open diamond) or T26 (filled square) for 7 (A), 14 (B), 30 (C), or 60 (D) days. Rats were killed at either activity onset (Hour 0) or activity offset, which varied according to the individual rat's activity pattern. Individual markers signify levels of PER2-ir versus time of perfusion for each rat.

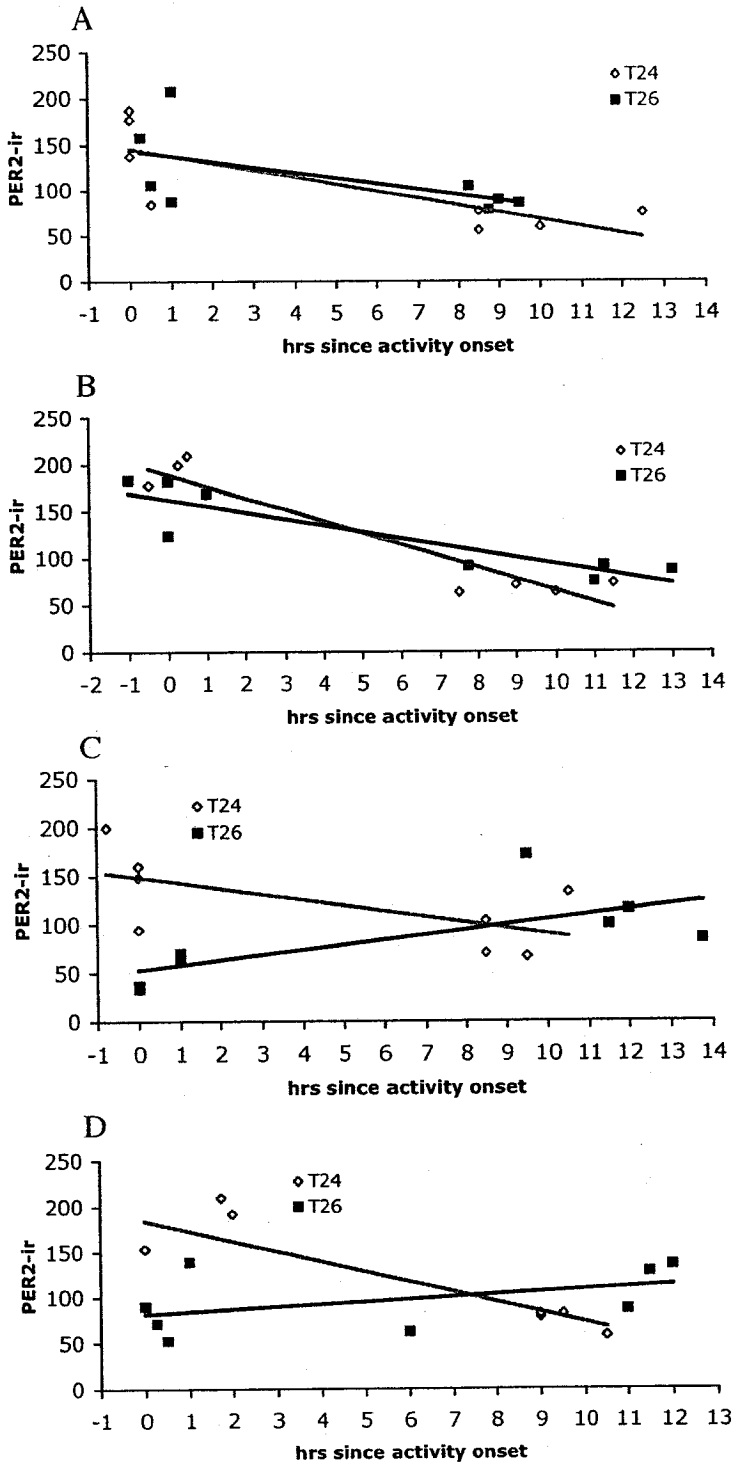

Figure A3. Scatterplot diagrams of PER2 immunoreactive cells in the CEA of individual rats under a T24 (open diamond) or T26 (filled square) for 7 (A), 14 (B), 30 (C), or 60 (D) days. Rats were killed at either activity onset (Hour 0) or activity offset, which varied according to the individual rat's activity pattern. Individual markers signify levels of PER2-ir versus time of perfusion for each rat.

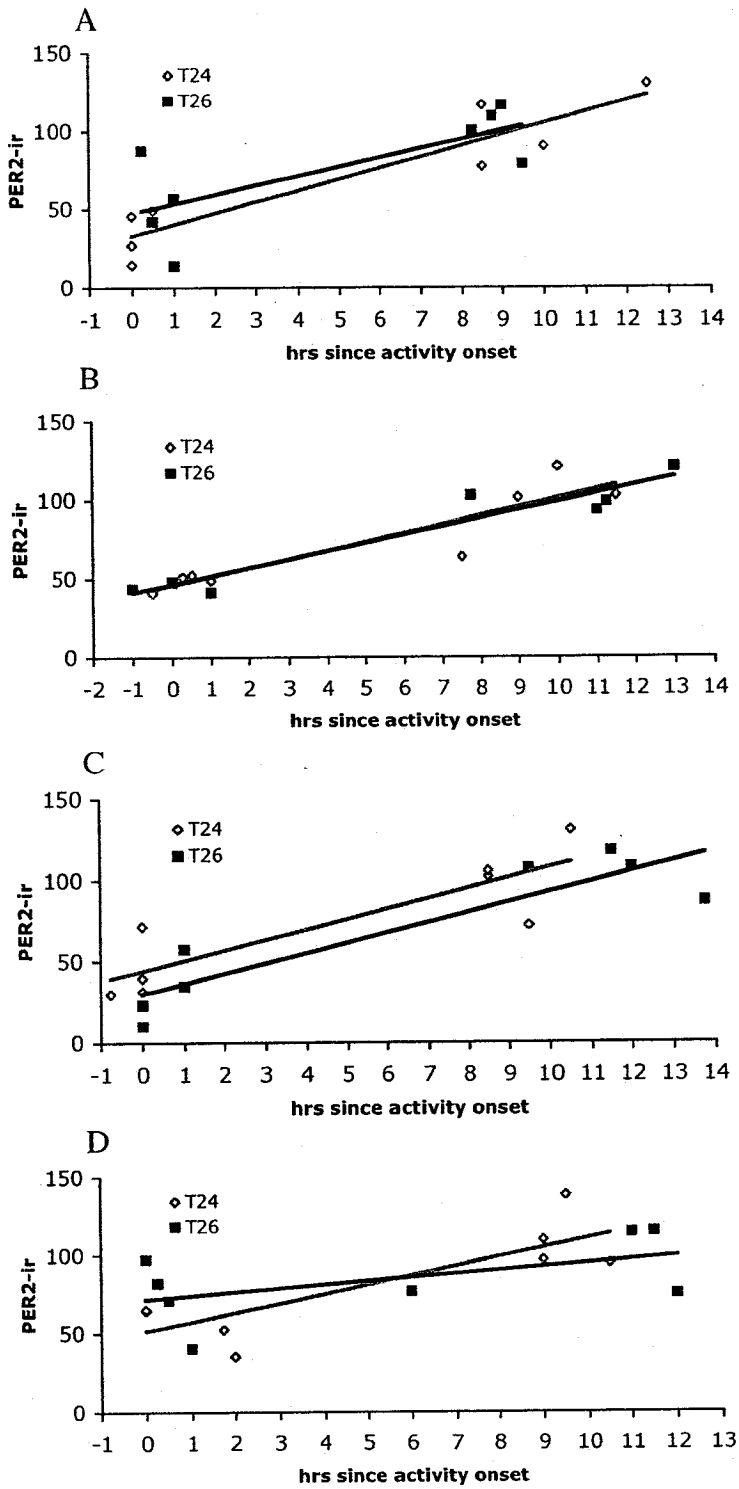

Figure A4. Scatterplot diagrams of PER2 immunoreactive cells in the BLA of individual rats under a T24 (open diamond) or T26 (filled square) for 7 (A), 14 (B), 30 (C), or 60 (D) days. Rats were killed at either activity onset (Hour 0) or activity offset, which varied according to the individual rat's activity pattern. Individual markers signify levels of PER2-ir versus time of perfusion for each rat.

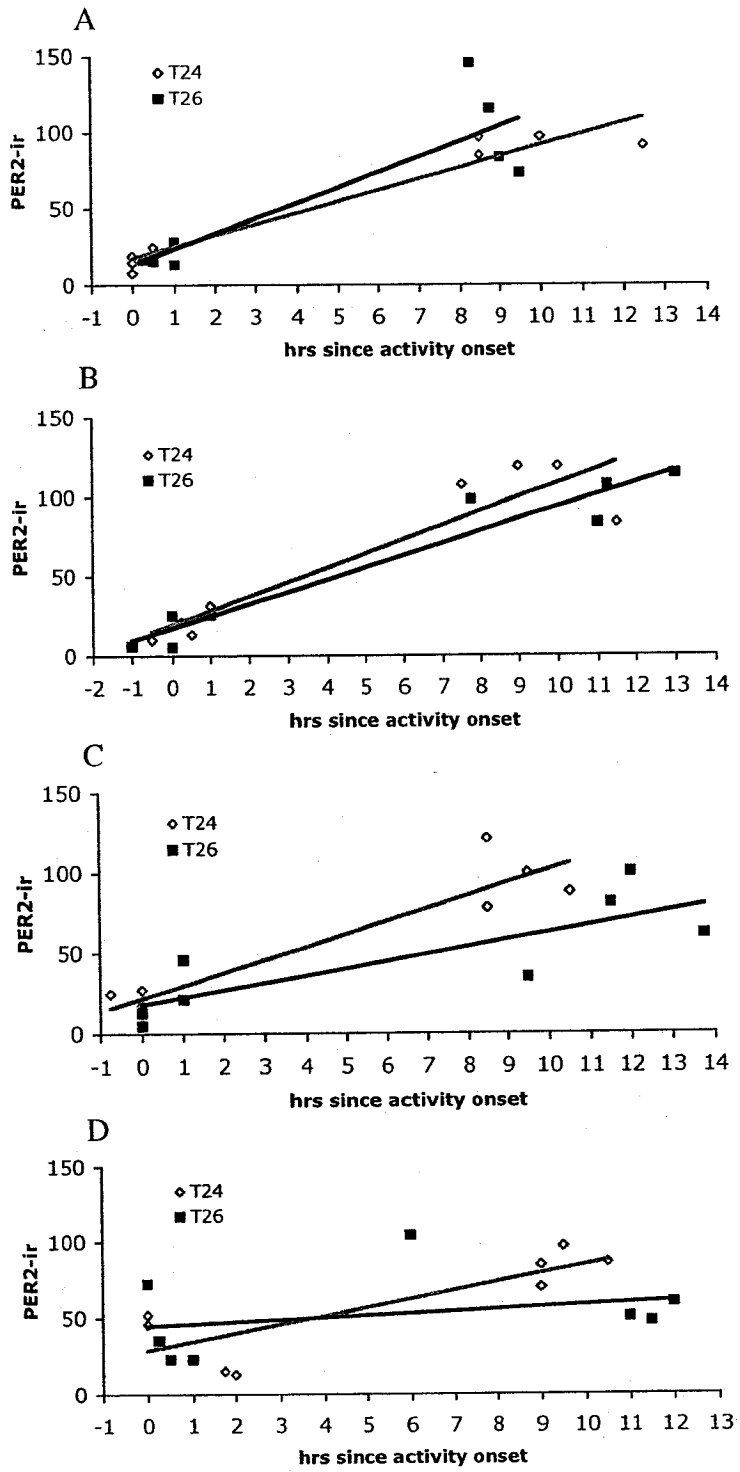

Figure A5. Scatterplot diagrams of PER2 immunoreactive cells in the DG of individual rats under a T24 (open diamond) or T26 (filled square) for 7 (A), 14 (B), 30 (C), or 60 (D) days. Rats were killed at either activity onset (Hour 0) or activity offset, which varied according to the individual rat's activity pattern. Individual markers signify levels of PER2-ir versus time of perfusion for each rat.

APPENDIX B

Table B1. Analysis of Variance for PER2-ir in the SCN of rats on a T24 or T26 cycle for 7, 14, 30, or 60 days and sacrificed at activity onset or offset.

Source	SS	df	MS	F	P
T-cycle	415.141	1	415.141	.245	.6227
Perfusion time (PT)	975008.131	1	975008.131	575.927	<.0001***
T-cycle * PT	375.391	1	375.391	.222	.6399
Day	9281.007	3	3093.669	1.827	.1548
T-cycle * Day	4306.317	3	1435.439	.848	.4746
PT * Day	14791.617	3	4930.539	2.912	.0438*
T-cycle * PT * Day	7501.597	3	2500.532	1.477	.2326
Error	81260.910	48	1692.936		

*: $p < .05$
**: $p < .01$
***: $p < .0001$

Table B2. Analysis of Variance for PER2-ir in the BNSTov of rats on a T24 or T26 cycle for 7, 14, 30, or 60 days and sacrificed at activity onset or offset.

Source	SS	df	MS	F	P
T-cycle	7284.622	1	7284.622	8.337	.0058**
Perfusion time (PT)	88268.410	1	88268.410	101.020	<.0001***
T-cycle * PT	28392.250	1	28392.250	32.494	<.0001***
Day	7405.483	3	2468.494	2.825	.0485*
T-cycle * Day	2512.722	3	837.574	.959	.4200
PT * Day	10888.315	3	3629.438	4.154	.0107**
T-cycle * PT * Day	9195.995	3	3065.332	3.508	.0222*
Error	41940.960	48	873.770		

*: $p < .05$
**: $p < .01$
***: $p < .0001$

Table B3. Analysis of Variance for PER2-ir in the CEA of rats on a T24 or T26 cycle for 7, 14, 30, or 60 days and sacrificed at activity onset or offset.

Source	SS	df	MS	F	P
T-cycle	3925.022	1	3925.022	4.264	.0444*
Perfusion time (PT)	41330.890	1	41330.890	44.899	<.0001***
T-cycle * PT	24680.410	1	24680.410	26.811	<.0001***
Day	4712.307	3	1570.769	1.706	.1782
T-cycle * Day	5654.408	3	1884.803	2.048	.1197
PT * Day	22975.490	3	7658.497	8.320	.0001***
T-cycle * PT * Day	7267.450	3	2422.483	2.632	.0606
Error	44185.780	48	920.537		

*: $p < .05$
**: $p < .01$
***: $p < .0001$

Table B4. Analysis of Variance for PER2-ir in the BLA of rats on a T24 or T26 cycle for 7, 14, 30, or 60 days and sacrificed at activity onset or offset.

Source	SS	df	MS	F	P
T-cycle	31.290	1	31.290	.083	.7745
Perfusion time (PT)	48485.288	1	48485.288	128.585	<.0001***
T-cycle * PT	184.790	1	184.790	.490	.4873
Day	1488.201	3	496.067	1.316	.2802
T-cycle * Day	267.786	3	89.262	.237	.8703
PT * Day	1697.179	3	565.726	1.500	.2264
T-cycle * PT * Day	1546.794	3	515.598	1.367	.2640
Error	18099.217	48	377.067		

*: $p < .05$
**: $p < .01$
***: $p < .0001$

Table B5. Analysis of Variance for PER2-ir in the DG of rats on a T24 or T26 cycle for 7, 14, 30, or 60 days and sacrificed at activity onset or offset.

Source	SS	df	MS	F	P
T-cycle	277.014	1	277.014	.852	.3605
Perfusion time (PT)	73308.947	1	73308.947	225.574	<.0001***
T-cycle * PT	590.794	1	590.794	1.818	.1839
Day	772.730	3	257.577	.793	.5040
T-cycle * Day	793.286	3	264.429	.814	.4926
PT * Day	5324.021	3	1774.674	5.461	.0026**
T-cycle * PT * Day	1064.031	3	354.677	1.091	.3618
Error	15599.417	48	324.988		

*: $p < .05$
**: $p < .01$
***: $p < .0001$

Table B6. Analysis of Variance for PER2-ir in the SCN of rats on a T24 or T26 cycle for 30 days and sacrificed at one of four time points; activity onset, onset +7hrs, activity offset, and offset +7hrs.

Source	SS	df	MS	F	P
T-cycle	233.863	1	233.863	.240	.6287
Perfusion time (PT)	221587.315	3	73862.438	75.720	<.0001***
T-cycle * PT	3246.105	3	1082.035	1.109	.3640
Error	24386.785	25	975.471		

*: $p < .05$
**: $p < .01$
***: $p < .0001$

Table B7. Analysis of Variance for PER2-ir in the BNSTov of rats on a T24 or T26 cycle for 30 days and sacrificed at one of four time points; activity onset, onset +7hrs, activity offset, and offset +7hrs.

Source	SS	df	MS	F	P
T-cycle	1062.103	1	1062.103	2.991	.0961
Perfusion time (PT)	18477.503	3	6159.168	17.342	<.0001***
T-cycle * PT	11930.972	3	3976.991	11.198	<.0001***
Error	8878.877	25	355.155		

*: $p < .05$
**: $p < .01$
***: $p < .0001$

Table B8. Analysis of Variance for PER2-ir in the CEA of rats on a T24 or T26 cycle for 30 days and sacrificed at one of four time points; activity onset, onset +7hrs, activity offset, and offset +7hrs.

Source	SS	df	MS	F	P
T-cycle	1886.401	1	1886.401	2.672	.1146
Perfusion time (PT)	27616.748	3	9205.583	13.041	<.0001***
T-cycle * PT	23163.521	3	7721.174	10.938	<.0001***
Error	17647.567	25	705.903		

*: $p < .05$
**: $p < .01$
***: $p < .0001$

Table B9. Analysis of Variance for PER2-ir in the BLA of rats on a T24 or T26 cycle for 30 days and sacrificed at one of four time points; activity onset, onset +7hrs, activity offset, and offset +7hrs.

Source	SS	df	MS	F	P
T-cycle	3085.155	1	3085.155	4.087	.0540
Perfusion time (PT)	12962.451	3	4320.817	5.724	.0040**
T-cycle * PT	1776.300	3	592.100	.784	.5139
Error	18871.557	25	754.862		

*: $p < .05$
**: $p < .01$
***: $p < .0001$

Table B10. Analysis of Variance for PER2-ir in the DG of rats on a T24 or T26 cycle for 30 days and sacrificed at one of four time points; activity onset, onset +7hrs, activity offset, and offset +7hrs.

Source	SS	df	MS	F	P
T-cycle	86.967	1	86.967	.408	.5288
Perfusion time (PT)	27074.033	3	9024.678	42.348	<.0001***
T-cycle * PT	3350.936	3	1116.979	5.241	.0061**
Error	5327.727	25	213.109		

*: $p < .05$
**: $p < .01$
***: $p < .0001$

APPENDIX C

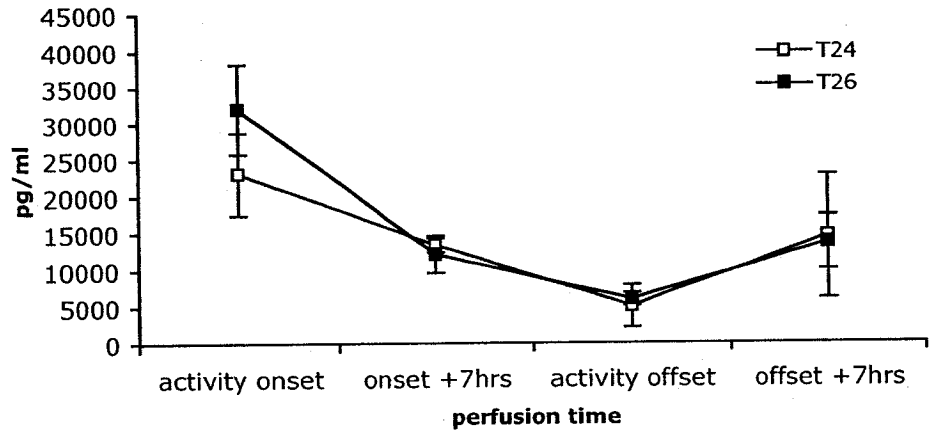

Figure C1. Mean (±SEM) corticosterone levels (pg/ml) in T24 (open square) and T26 (filled square) rats after 30 days on a T-cycle and sacrificed at either activity onset, onset +7hrs, activity offset, or offset +7hrs. N equals 3-5/group.